© 2014. Published by The Company of Biologists Ltd | Development (2014) 141, 3540-3550 doi:10.1242/dev.111294

RESEARCH ARTICLE

Cdk5 and its substrates, Dcx and p27kip1, regulate cytoplasmic dilation formation and nuclear elongation in migrating neurons

Yoshiaki V. Nishimura[1,2,3], Mima Shikanai[1,4], Mikio Hoshino[5], Toshio Ohshima[6], Yo-ichi Nabeshima[7], Ken-ichi Mizutani[2], Koh-ichi Nagata[3], Kazunori Nakajima[1] and Takeshi Kawauchi[1,4,8,*]

ABSTRACT

Neuronal migration is crucial for development of the mammalian-specific six-layered cerebral cortex. Migrating neurons are known to exhibit distinct features; they form a cytoplasmic dilation, a structure specific to migrating neurons, at the proximal region of the leading process, followed by nuclear elongation and forward movement. However, the molecular mechanisms of dilation formation and nuclear elongation remain unclear. Using *ex vivo* chemical inhibitor experiments, we show here that rottlerin, which is widely used as a specific inhibitor for PKCδ, suppresses the formation of a cytoplasmic dilation and nuclear elongation in cortical migrating neurons. Although our previous study showed that cortical neuronal migration depends on Jnk, another downstream target of rottlerin, Jnk inhibition disturbs only the nuclear elongation and forward movement, but not the dilation formation. We found that an unconventional cyclin-dependent kinase, Cdk5, is a novel downstream target of rottlerin, and that pharmacological or knockdown-mediated inhibition of Cdk5 suppresses both the dilation formation and nuclear elongation. We also show that Cdk5 inhibition perturbs endocytic trafficking as well as microtubule organization, both of which have been shown to be required for dilation formation. Furthermore, knockdown of Dcx, a Cdk5 substrate involved in microtubule organization and membrane trafficking, or p27kip1, another Cdk5 substrate involved in actin and microtubule organization, disturbs the dilation formation and nuclear elongation. These data suggest that Cdk5 and its substrates, Dcx and p27kip1, characterize migrating neuron-specific features, cytoplasmic dilation formation and nuclear elongation in the mouse cerebral cortex, possibly through the regulation of microtubule organization and an endocytic pathway.

KEY WORDS: Cell migration, Cytoskeleton, Endocytosis, C-jun N-terminal kinase, Doublecortin, Rab5, Mouse, Cdkn1b

INTRODUCTION

During organogenesis, newly generated cells from the progenitors are allocated on the basis of their subtypes or properties to construct sophisticated tissue structures. Because tissue stem cells and progenitors are spatially restricted in many organs, including developing brains, differentiating cells need to migrate to their final destinations. Cell migration patterns can be classified according to cell type. Epithelial cells exhibit a collective cell migration, whereas fibroblasts display a mesenchymal single cell migration (Kawauchi, 2012). Nevertheless, these two different types of migrating cells share some common features. Migrating (or leading) cells extend filopodia and lamellipodia, and form a new adhesion to the extracellular matrix, followed by nuclear forward movement. These cellular events are controlled by Rho family small GTPases, such as Rac1, Cdc42 and RhoA (Nobes and Hall, 1995).

By contrast, migrating neurons undergo unique morphological changes. They extend a thick neurite, called a leading process, and form a 'cytoplasmic dilation' (also known as a 'swelling') at the proximal region of the leading process (Bellion et al., 2005; Schaar and McConnell, 2005). Subsequently, the nucleus elongates and moves into the dilation. The cytoplasmic dilation is a distinctive subcellular domain, observed only in migrating neurons, not in other migrating cells such as fibroblasts and neutrophils (Schaar and McConnell, 2005). Therefore, it is believed that a neuron-specific molecule may control the formation of cytoplasmic dilations. However, such a molecule has not been identified, although a recent study revealed that Rac1 and its interacting protein POSH (Sh3rf1 – Mouse Genome Informatics) are required for dilation formation (Yang et al., 2012).

Cyclin-dependent kinase 5 (Cdk5) is an unconventional CDK protein, because it is predominantly activated in post-mitotic neurons rather than in dividing neural progenitors (Tsai et al., 1993; Kawauchi et al., 2013). In addition, unlike conventional CDKs, Cdk5 activity is not dependent on cyclins, but is controlled by its specific activators, p35 or p39 (Hisanaga and Saito, 2003). Consistent with its high activity in neurons, Cdk5 controls the early phases of neuronal migration in the developing brains mainly through the regulation of microtubules and actin cytoskeleton (Niethammer et al., 2000; Tanaka et al., 2004b; Kawauchi et al., 2006).

In the developing cerebral cortex, neurons exhibit multi-step modes of neuronal migration, of which the locomotion mode is a major one as it covers most of the neuronal path (Rakic, 1972; Nadarajah and Parnavelas, 2002). However, it is difficult to analyze the locomotion mode without dealing with the secondary defects derived from the early phase of migration, because inhibition of many molecules, including Cdk5 and Rac1, leads to defects in the early phase of migration (Ayala et al., 2007; Kawauchi and Hoshino, 2008; Govek et al., 2011). We recently established a novel *ex vivo* chemical inhibitor assay, which allows us to directly analyze the locomotion mode of neuronal migration (Nishimura et al., 2010). Using this novel technique, we showed that rottlerin, widely used as a specific inhibitor for protein kinase C delta (PKCδ),

[1]Department of Anatomy, Keio University School of Medicine, 35 Shinanomachi, Shinjuku-ku, Tokyo 160-8582, Japan. [2]Laboratory of Neural Differentiation, Graduate School of Brain Science, Doshisha University, 4-1-1 Kizugawa-dai, Kizugawa-shi, Kyoto 619-0225, Japan. [3]Department of Molecular Neurobiology, Institute for Developmental Research, Aichi Human Service Center, 713-8 Kamiya, Kasugai, Aichi 480-0392, Japan. [4]Department of Physiology, Keio University School of Medicine, 35 Shinanomachi, Shinjuku-ku, Tokyo 160-8582, Japan. [5]Department of Biochemistry and Cellular Biology, National Institute of Neuroscience, NCNP, Tokyo 187-8502, Japan. [6]Department of Life Science and Medical Bioscience, Waseda University, Tokyo 162-8430, Japan. [7]Laboratory of Molecular Life Science, Foundation for Biomedical Research and Innovation, Kobe 650-0047, Japan. [8]Precursory Research for Embryonic Science and Technology (PRESTO), Japan Science and Technology Agency (JST), Saitama 332-0012, Japan.

*Author for correspondence (takeshi-kawauchi@umin.ac.jp)

Received 10 April 2014; Accepted 16 July 2014

Development (2014) 141, 3540-3550 doi:10.1242/dev.111294

suppresses the nuclear movement of the locomoting neurons partly via the inhibition of the activity of a novel downstream target molecule, c-jun N-terminal kinase (Jnk) (Nishimura et al., 2010).

In this study, we show that rottlerin treatment disturbs the cytoplasmic dilation formation and nuclear elongation of migrating neurons. Interestingly, however, inhibition of Jnk has little effects on dilation formation. We found that Cdk5/p35 is a novel downstream target of rottlerin, and that Cdk5 is required for the formation of cytoplasmic dilation and nuclear morphological changes, possibly through the regulation of microtubule organization and an endocytic pathway. These observations indicate that Cdk5, which is predominantly activated in post-mitotic neurons, characterizes the neuron-specific migration pattern through regulation of cytoplasmic dilation formation and nuclear elongation.

RESULTS

Rottlerin suppresses the cytoplasmic dilation formation and nuclear elongation

Our *ex vivo* chemical inhibitor screens previously found that treatment with rottlerin strongly suppresses the locomotion mode of neuronal migration in slice-cultured cerebral cortices, partly through the inhibition of a novel downstream target, Jnk, but not through inhibition of PKCδ (Nishimura et al., 2010). This led us to investigate the effects of rottlerin on cytoplasmic dilation formation and nuclear morphological changes in the cortical slices. Mouse cerebral cortices were electroporated *in vivo* with EGFP- and nuclear localizing signal (NLS)-fused DsRed-expressing vectors at embryonic day 14 (E14), and the electroporated brains were subjected to slice culture at E16. Time-lapse analyses showed that the locomoting neurons formed a cytoplasmic dilation at the proximal region of the leading process and subsequently exhibited nuclear elongation to enter the dilation in the control cortical slices (Fig. 1A; supplementary material Fig. S1A,C and Movie 1) (Bellion et al., 2005; Schaar and McConnell, 2005; Tsai et al., 2007). By contrast, in the rottlerin-treated cortical slices, cytoplasmic dilation was greatly perturbed in the locomoting neurons (Fig. 1A; supplementary material Fig. S1B,C and Movie 2). The ratio of cells displaying a cytoplasmic dilation was dramatically reduced 3 h after rottlerin treatment (Fig. 1B). At the same time-point, the nuclei in the rottlerin-treated cells appeared round in shape, whereas many control cells exhibited elongated nuclear morphologies (Fig. 1C). The ratio of length to width of the nuclei was significantly reduced in the rottlerin-treated cortical slices at 3 and 8 h after rottlerin treatment, compared with that of control (Fig. 1D).

Jnk regulates nuclear elongation, but not dilation formation

Rottlerin has generally been used as a specific inhibitor for PKCδ (Gschwendt et al., 1994; Kang et al., 2013). However, our previous

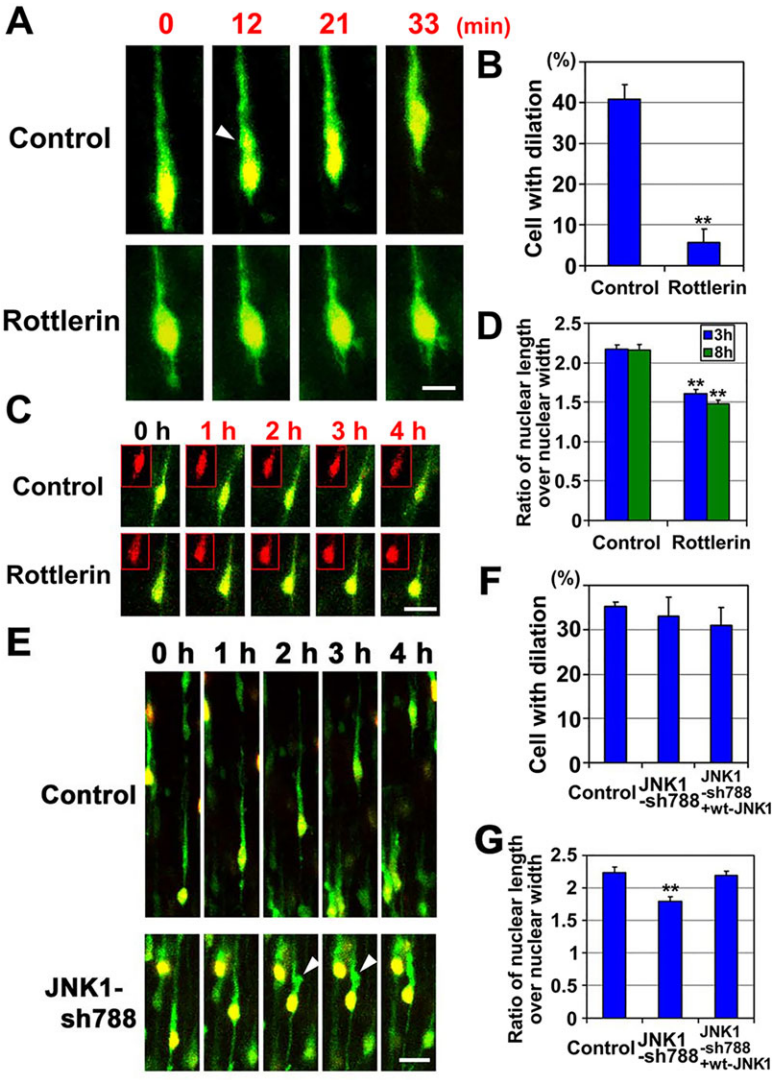

Fig. 1. Rottlerin treatment suppresses the formation of the cytoplasmic dilation in a Jnk-independent manner. (A) Time-lapse observation of the locomoting neurons in cultured cortical slices with or without rottlerin (5 μM). At 0 min (shown in red), treatment with an inhibitor had already taken place (time=0 min: 30 min after inhibitor treatment). White arrowhead indicates a cytoplasmic dilation and the nucleus entering the dilation (yellow). (B) Ratios of cells with a cytoplasmic dilation 3 h after inhibitor treatment. *n*=40 (control) or 49 (rottlerin) cells (from four slices). (C) Time-lapse observation of locomoting neurons in cultured cortical slices with or without rottlerin (5 μM). Cortical slices were treated with rottlerin or solvent (control) just after 0 h. The insets show nuclear morphologies, visualized by NLS-DsRed-mediated fluorescence. (D) Ratios of length to width of the nuclei in locomoting neurons 3 or 8 h after inhibitor treatment. Control, *n*=36 cells (three slices); rottlerin, *n*=34 (3 h) and 36 (8 h) cells (three slices). (E) Time-lapse observation of control or Jnk1-knockdown locomoting neurons. White arrowheads indicate the cytoplasmic dilation. (F) Ratio of cells with a cytoplasmic dilation. Control, *n*=46 cells (four slices); Jnk1-sh788, *n*=49 cells (five slices); Jnk1-sh788+wt-Jnk1, *n*=58 cells (five slices). No significant difference between control and Jnk1-sh788 was found using Student's *t*-test. (G) Ratios of length to width of nuclei in Jnk1-knockdown locomoting neurons. Control, Jnk1-sh788 and Jnk1-sh788+wt-Jnk1: *n*=30 cells (three slices). Data are mean±s.e.m. Significance of differences between control and inhibitor treatment or knockdown was determined using Student's *t*-test. $^{**}P<0.01$. Scale bars: 10 μm in A; 20 μm in C,E.

Development (2014) 141, 3540-3550 doi:10.1242/dev.111294

study indicated that, in contrast to rottrelin treatment, knockdown of PKCδ does not affect the locomotion mode of neuronal migration, and that rottlerin also inhibits Jnk activity, which is required for the locomotion (Nishimura et al., 2010). Therefore, we next examined the involvement of Jnk in the formation of the cytoplasmic dilation.

We constructed a short hairpin RNA (shRNA)-based knockdown vector for Jnk1-coding sequence (Jnk1-sh788), and confirmed that this shRNA efficiently reduced endogenous Jnk1 protein levels in primary cortical neurons 2 days after transfection (supplementary material Fig. S2A). We then electroporated Jnk1-sh788 into mouse embryonic cerebral cortices at E14 and the electroporated brains were subjected to slice culture at E16. The Jnk1 knockdown resulted in delayed nuclear movements and abnormal leading process morphologies in locomoting neurons (Fig. 1E and supplementary material Fig. S3E), as previously reported (Kawauchi et al., 2003; Nishimura et al., 2010). To our surprise, however, these locomoting neurons formed a cytoplasmic dilation to a similar extent to that in control, although their morphologies were rough and irregular in parts (Fig. 1F). By contrast, their nuclear elongation was disrupted, which was rescued by co-expression of human wt-Jnk1 (Fig. 1G). In our *ex vivo* chemical inhibitor assay, a Jnk inhibitor, SP600125, also showed similar results to Jnk1 knockdown (supplementary material Fig. S3A-D). These results suggest that Jnk is required for the nuclear elongation and forward movement but is dispensable for dilation formation in the locomoting neurons. It further suggests that other rottlerin-target molecule(s) may be involved in the formation of the cytoplasmic dilation.

Identification of Cdk5 as a novel downstream target of rottlerin

We subsequently searched for a novel molecular pathway suppressed by rottlerin treatment, and found that rottlerin decreased the phosphorylation of focal adhesion kinase (FAK) at Ser732 (Fig. 2A). It is known that the Ser732 residue on FAK is specifically phosphorylated by Cdk5, because Ser732 phosphorylation disappears in the Cdk5-knockout cerebral cortex (Xie et al., 2003). Furthermore, protein levels of a Cdk5-specific activator, p35, which is also phosphorylated by Cdk5 (Asada et al., 2012), are reduced in the rottlerin-treated cortical neurons (Fig. 2A). By contrast, treatment with bisindolylmaleimide I (BIM), a chemical inhibitor for all PKC proteins, including PKCδ, did not affect either Ser732 phosphorylation of FAK or p35 protein levels, suggesting that rottlerin inhibits a molecule upstream of Cdk5/p35, independently of PKCδ suppression. These data suggest that rottlerin indirectly decreases Cdk5 activity. Our previous data showed that inhibition of Cdk5 does not decrease Jnk activity (Kawauchi et al., 2005), but suppresses the locomotion mode of neuronal migration (Nishimura et al., 2010), suggesting that Cdk5 may have a function in locomoting neurons in a Jnk-independent manner.

Cdk5 regulates the formation of cytoplasmic dilation and nuclear elongation

To elucidate the role of Cdk5 in locomotion, we applied a CDK inhibitor, roscovitine (Meijer et al., 1997), in our *ex vivo* chemical inhibitor assay. Cytoplasmic dilation formation in neurons in the roscovitine-treated cortical slices was severely affected (Fig. 2B; supplementary material Fig. S4 and Movie 3). The ratio of the cells with dilations was significantly reduced 3 h after roscovitine treatment (Fig. 2C), and nuclei exhibited round morphologies (Fig. 2D,E). More-detailed analyses revealed that control locomoting neurons exhibited a saltatory movement, as previously reported (Edmondson and Hatten, 1987; Schaar and McConnell, 2005); after the peak of the migration speed per unit, the sphericity of the nucleus was increased, i.e. the nucleus became rounded (Fig. 3A). By contrast, although the

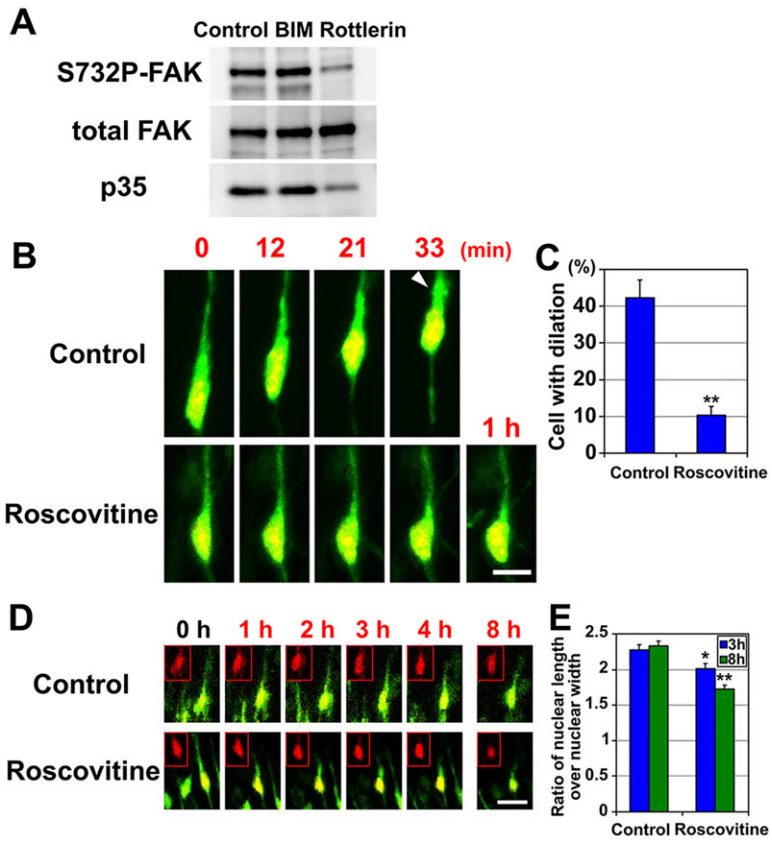

Fig. 2. Identification of the Cdk5 pathway as a novel downstream target of rottlerin. (A) Primary cortical neurons from E15 cerebral cortices were incubated for 2 days *in vitro* and treated with the indicated inhibitors for 3 h. Immunoblot analyses of cell lysates with indicated antibodies were performed. (B) Time-lapse observation of the locomoting neurons in cultured cortical slices with or without roscovitine (100 μM). At 0 min (shown in red), treatment with an inhibitor had already taken place (time=0 min: 30 min after inhibitor treatment). White arrowhead indicates a cytoplasmic dilation. (C) Ratios of cells with a cytoplasmic dilation 3 h after inhibitor treatment. Control, *n*=33 cells (from four slices); roscovitine, *n*=86 cells (five slices). (D) Time-lapse observation of locomoting neurons in cortical slices with or without roscovitine (100 μM). Cortical slices were treated with inhibitor just after 0 h. The insets show nuclear morphologies, visualized by NLS-DsRed-mediated fluorescence. (E) Ratios of length to width of nuclei in locomoting neurons 3 or 8 h after inhibitor treatment. Control, *n*=30 cells (three slices); roscovitine, *n*=50 (3 h) and 37 (8 h) cells (three slices). Data are mean±s.e.m. Significance of differences was determined using Student's *t*-test. **P*<0.05, ***P*<0.01. Scale bars: 10 μm in B; 20 μm in D.

Development (2014) 141, 3540-3550 doi:10.1242/dev.111294

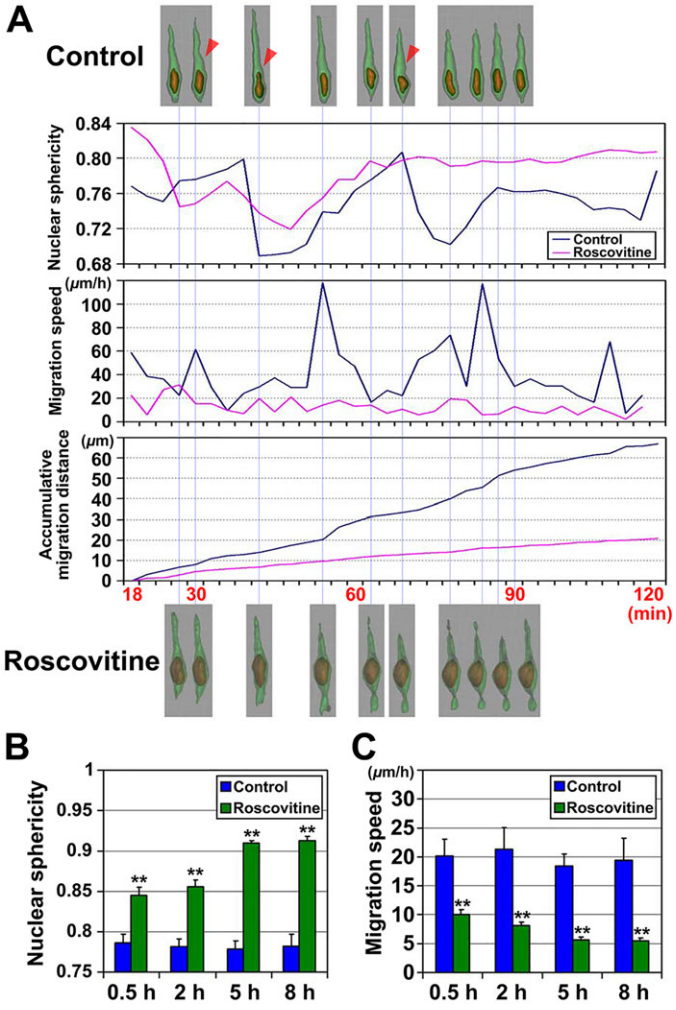

Fig. 3. The effects of roscovitine treatment on the saltatory movement of the locomoting neurons. (A) The nuclear sphericity, migration speed per unit (μm/h) and accumulative migration distances (μm) of control (blue lines) or roscovitine-treated locomoting neurons (magenta lines) are plotted by DippMotion 2D and Imaris software with some modification by Excel. 'Sphericity=1' means completely round. The migration speed was calculated every 3 min. The *x*-axis shows the number of minutes after inhibitor treatment. Red arrowheads in the extracted images, traced by Imaris software, indicate cytoplasmic dilations. (B,C) The sphericity of nuclei (B) or migration speed (C) at the indicated time after inhibitor treatment. Data are mean of ratios±s.e.m. Control, n=20 (0.5 h), 14 (2 h), 10 (5 h) and 10 (8 h) cells (three slices); roscovitine, n=25 (0.5 h), 30 (2 h), 30 (5 h) and 30 (8 h) cells (three slices). Significance of differences was determined using Welch's t-test. **P<0.01.

migration speed of the neurons in the roscovitine-treated cortical slices remained constantly low, the nuclear sphericity increased continuously from 30 min after roscovitine treatment (Fig. 3A-C). The nuclear sphericity gradually increased as nuclear movement abated (Fig. 3A), but even 30 min after roscovitine treatment, the rounding of the nucleus was significantly higher than that of control (Fig. 3B), suggesting that at least in part, Cdk5 actively regulates nuclear morphological changes. This is consistent with a previous report that Cdk5-mediated phosphorylation of Ser732 on FAK regulates the nuclear morphological changes (Xie et al., 2003).

It has been reported that roscovitine is a reliable specific inhibitor for CDK proteins (Meijer et al., 1997; Bain et al., 2003, 2007), but from these experiments it is unclear whether the effects of roscovitine are cell-autonomous or not. To test this and confirm our inhibitor experiments, we performed knockdown experiments using Cdk5-shRNA-expressing vectors (Cdk5-sh250) (Kawauchi et al., 2006) (supplementary material Fig. S2B). Because Cdk5 also has important roles in the early phase of neuronal migration (Kawauchi et al., 2006; Ohshima et al., 2007), most Cdk5-knockdown neurons are unable to transition into the locomotion mode, but a small fraction enter the cortical plate exhibiting locomoting morphologies (Fig. 4A,F). These Cdk5-knockdown locomoting neurons showed delayed migration as we have previously reported (Nishimura et al., 2010), suggesting that the Cdk5 activity is at least partially suppressed in these neurons even after the transition to the locomotion mode (Fig. 4A). Therefore, we analyzed the morphologies of these Cdk5-knockdown locomoting neurons. Consistent with the inhibitor experiments, the ratio of the cells with a cytoplasmic dilation was dramatically reduced and nuclear elongation was significantly disturbed in the Cdk5-sh250-electroporated cortical slices; these phenotypes were rescued by the co-expression of human wt-Cdk5 (Fig. 4A-D). The area occupied by leading processes 10 μm from the cell soma, which corresponds to the dilation, was decreased in the Cdk5, but not Jnk1, knockdown neurons (Fig. 4E). These data suggest that Cdk5 cell-autonomously regulates the formation of cytoplasmic dilation and nuclear morphological changes.

To confirm these results *in vivo*, we examined the involvement of Cdk5 in dilation formation in fixed cortical sections. Cdk5-sh250 was electroporated into embryonic cerebral cortex at E14, and the electroporated brains were harvested and examined at E17. A small fraction of Cdk5-knockdown neurons exhibited locomoting morphologies, but very little cytoplasmic dilation was observed (Fig. 4F,G). Taken together, these results indicate that Cdk5, but not Jnk, is essential for formation of the cytoplasmic dilation.

Cdk5 controls microtubule organization and endocytic trafficking

We next examined the events downstream of Cdk5 that might regulate dilation formation in locomoting neurons. Previous electron microscopy analyses showed that a dilation/swelling contains Golgi apparatus, clathrin-coated pits and abundant microtubules elongating from a centrosome (Bellion et al., 2005; Schaar and McConnell, 2005; Shieh et al., 2011). Cdk5-knockdown or roscovitine-treated primary cortical neurons exhibited abnormal microtubule orientations surrounding the nuclei (Fig. 5A; supplementary material Figs S5A,B and S6). Roscovitine seemed to perturb Golgi localization in primary cortical neurons. Furthermore, the distance between the electroporated Golgi-localized EYFP and the nucleus was decreased in the locomoting neurons in the roscovitine-treated cortical slices (supplementary material Fig. S5C,D). The distance between the GM130-positive *cis*-Golgi and nucleus was also decreased in fixed cortical sections, possibly owing to lower motility of the Golgi in the Cdk5-knockdown locomoting neurons (Fig. 5B and supplementary material Fig. S5E).

We next examined the involvement of Cdk5 in clathrin-mediated endocytic pathways by using a transferrin (Tf) uptake assay. It is known that Tf that is internalized via clathrin-mediated endocytosis is transported to Rab5-positive early endosomes and subsequently to Rab11-positive perinuclear recycling endosomes (Ullrich et al., 1996; Trischler et al., 1999). Primary cortical neurons were transfected with Cdk5-sh250 or control vectors, and treated with Alexa594-conjugated Tf (Tf-594) for 10 or 30 min. By 10 min after the treatment, Tf-594-mediated signals displayed dot-like patterns in both control and Cdk5-knockdown neurons (Fig. 5C, upper panels). While Tf-594 was transported to perinuclear regions

Development (2014) 141, 3540-3550 doi:10.1242/dev.111294

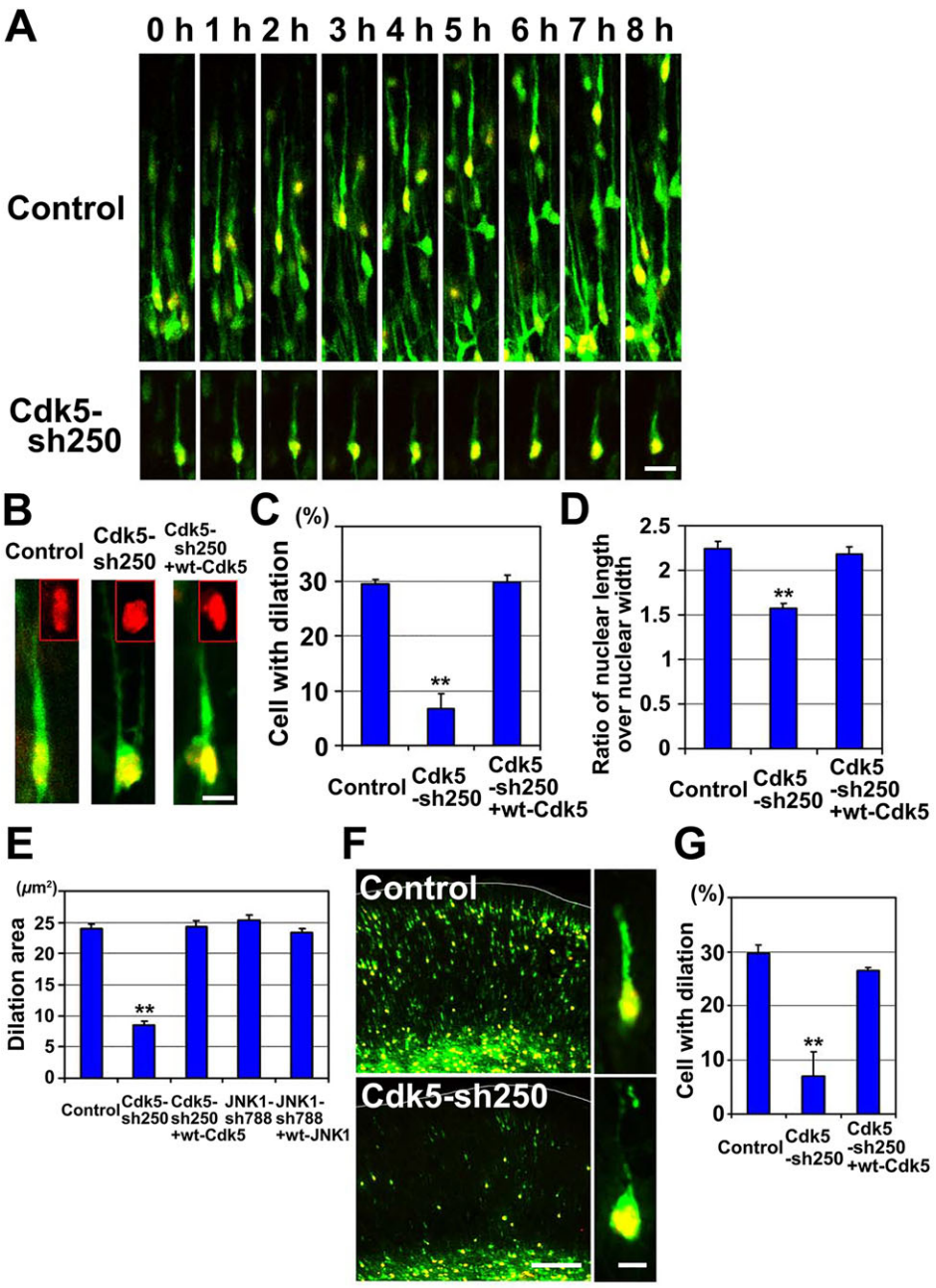

Fig. 4. Knockdown of Cdk5 suppresses the formation of a cytoplasmic dilation and nuclear elongation. (A) Time-lapse observation of control or Cdk5-knockdown locomoting neurons. (B) Representative images of control or Cdk5-knockdown or Cdk5-knockdown-rescued locomoting neurons. The insets show nuclear morphologies, visualized by NLS-DsRed-mediated fluorescence. (C,G) Ratios of cells with a cytoplasmic dilation in cortical slice cultures (C) or *in vivo* cortical sections (G). (C) Control, *n*=44 cells (four slices); Cdk5-sh250, *n*=33 cells (five slices); Cdk5-sh250+wt-Cdk5, *n*=44 cells (four slices). (G) Control, *n*=47 cells (four sections); Cdk5-sh250, *n*=44 cells (four sections); Cdk5-sh250 +wt-Cdk5, *n*=83 cells (four sections). (D) Ratio of length to width of nuclei in Cdk5-knockdown locomoting neurons. Control, Cdk5-sh250 and Cdk5-sh250+wt-Cdk5, *n*=30 cells (three slices). (E) The dilation area (see Materials and Methods) in Cdk5- or Jnk1-knockdown locomoting neurons. Control and Cdk5-sh250+ wt-Cdk5, *n*=10 cells (three slices); Cdk5-sh250, *n*=10 cells (six slices); Jnk1-sh788 and Jnk1-sh788+wt-Jnk1, *n*=10 cells (four slices). (F) Cryosections of control or Cdk5-knockdown vector-electroporated cerebral cortices at E17, 3 days after *in vivo* electroporation. Right panels are high-magnification images. Co-electroporated EGFP and NLS-DsRed signals are shown. Data are mean±s.e.m. Significance of differences was determined using Student's *t*-test. ***P*<0.01. Scale bars: 20 μm in A; 10 μm in B; 5 μm in the right panels in F; 100 μm in the left panels in F.

30 min after Tf-594 treatment in control neurons, as previously reported (Kawauchi et al., 2010), Tf-594-mediated signals remained as dot-like patterns 30 min after treatment in Cdk5-knockdown neurons (Fig. 5C, lower panels). The ratio of cells with perinuclear accumulation was significantly decreased in Cdk5-knockdown neurons (Fig. 5D). The dot-like staining in Cdk5-knockdown neurons 30 min after Tf-594 treatment was partially colocalized with transfected EGFP-Rab5, a marker for early endosomes, suggesting that Cdk5 regulates the endocytic pathway at early endosomes (Fig. 5E).

These results were supported by inhibitor experiments. Primary cortical neurons, transfected with EGFP-Rab5 as a marker for early endosomes, were treated with roscovitine or control solvent for 60 min, and additionally treated with Tf-594 for 10 or 30 min. Similar to the knockdown experiments, roscovitine treatment suppressed the Tf-594 transport (supplementary material Fig. S7). These results suggest that suppression of Cdk5 eventually results in inhibition of the endocytic trafficking pathway from clathrin-mediated endocytosis to the perinuclear endosomes in embryonic cortical neurons.

Inhibition of endocytic trafficking disturbs dilation formation and nuclear elongation

We have previously reported that Rab5-dependent endocytosis, comprising almost all clathrin-mediated endocytosis, and Rab11-dependent recycling are essential for neuronal migration (Kawauchi et al., 2010), but the roles of endocytic pathways in the cytoplasmic dilation formation and nuclear elongation remained unclear. Because *in vivo* electroporation-mediated inhibition of Dynamin results in cell death 3 days after electroporation (Kawauchi et al., 2010), we used an *ex vivo* chemical inhibitor assay to bypass the abnormalities at the early phase of neuronal migration.

Dynasore is a specific inhibitor for dynamin 1 and dynamin 2, both of which are essential for many types of endocytosis, including

Development (2014) 141, 3540-3550 doi:10.1242/dev.111294

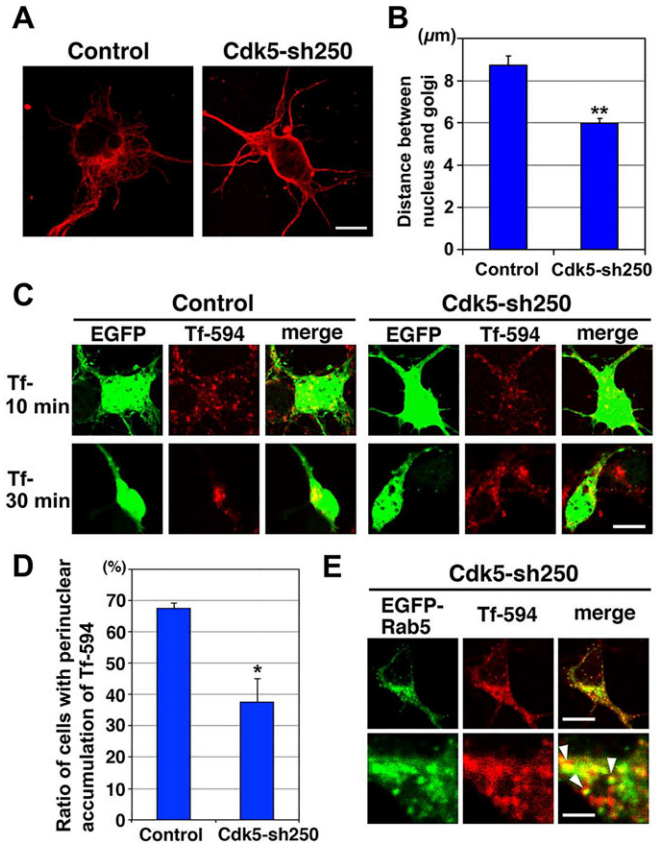

Fig. 5. Cdk5 controls microtubule morphologies, Golgi localization and an endocytic pathway. (A) Primary cortical neurons from E15 cerebral cortices were transfected with the indicated plasmids and incubated for 2 days *in vitro*. Cells were stained with anti-EGFP and anti-β-tubulin (red) antibodies, and DAPI. EGFP and DAPI staining signals are shown in supplementary material Fig. S6. (B) Distances between the center of the Golgi (GM130) and nucleus (DAPI) in the locomoting neurons in frozen cortical sections. Control, n=17 cells (from 13 sections); Cdk5-sh250, n=13 cells (11 sections). (C,E) Primary cortical neurons from E15 cerebral cortices were transfected with the indicated plasmids and EGFP- (C) or EGFP-Rab5-expressing vectors (E), incubated for 2 days *in vitro* and treated with Alexa594-conjugated transferrin (Tf-594) for 10 or 30 min before fixation. White arrowheads indicate colocalization of EGFP-Rab5 and Tf-594. (D) Ratios of cells with perinuclear accumulation of Tf-594. n=3 experiments (control, 61 cells; roscovitine, 86 cells). Data are mean±s.e.m. Significance of differences was determined using Student's t-test. *P<0.05, **P<0.01. Scale bars: 10 μm in A; 10 μm in C and the upper panels in E; 2.5 μm in the lower panels in E.

clathrin-mediated endocytosis (Macia et al., 2006). When cortical slices were treated with 80 μM of dynasore, we found that the locomotion mode of neuronal migration was strongly inhibited (data not shown). However, at this concentration, dynasore has been reported to inhibit a mitochondrial dynamin-related protein, Drp1, as well as endocytic dynamin 1 and dynamin 2 (Macia et al., 2006). Therefore, in this study, we used a lower concentration of 40 μM of dynasore to suppress endocytic trafficking.

Cerebral cortices were electroporated with EGFP- and NLS-fused DsRed-expressing vectors at E14, and the electroporated brains were subjected to slice culture at E16. Treatment with dynasore delayed the nuclear movement in the locomoting neurons (Fig. 6A,B), as previously reported (Wilson et al., 2010), and also decreased both the ratio of cells with a cytoplasmic dilation and the ratio of length to width of the nuclei (Fig. 6C-E; supplementary material Movie 4). Furthermore, knockdown-mediated inhibition of Rab5 also disturbed dilation formation and nuclear elongation, both of which were rescued by co-expression of human wt-Rab5 (Fig. 6F-H). These data suggest that endocytic pathways are required for the formation of cytoplasmic dilation and nuclear elongation during the locomotion mode of neuronal migration.

Microtubule organization is required for dilation formation and nuclear elongation

To examine the involvement of microtubule organization in dilation formation, cortical slices were treated with 100 nM nocodazole, an inhibitor of microtubule polymerization. Nocodazole treatment resulted in decrease of the ratio of cells with dilation and with elongated nucleus, suggesting that microtubule organization as well as endocytic trafficking are required for dilation formation and nuclear elongation during the locomotion mode of migration (Fig. 7).

Because F-actin is concentrated at the proximal region of the leading process in migrating cerebellar granule neurons (Solecki et al., 2009), we analyzed actin dynamics using time-lapse imaging of the electroporated EGFP-actin. In control locomoting neurons, strong EGFP-actin signals were observed above the nucleus or proximal region of the leading process before nuclear movement (supplementary material Fig. S8), consistent with a previous report (Solecki et al., 2009). By contrast, strong EGFP-actin accumulation was hardly detected in the Cdk5-knockdown neurons. However, both control and Cdk5-knockdown neurons sometimes extended lamellipodia-like structures (supplementary material Fig. S8). Therefore, Cdk5 suppression did not completely inhibit actin dynamics in the locomoting neurons. We next tried to inhibit actin dynamics by treatment with cytochalasin D or latrunculin B, both of which inhibit actin polymerization. However, because both drugs induced disruption of cortical slice tissues (supplementary material Movies 5 and 6), we could not analyze the effect of actin dynamics on dilation formation.

Dcx and p27^{kip1} control dilation formation and nuclear elongation

Cdk5 is known to phosphorylate many substrate molecules (Kawauchi, 2014). One of them, Doublecortin (Dcx), is involved in microtubule polymerization, membrane trafficking and actin organization (Francis et al., 1999; Gleeson et al., 1999; Friocourt et al., 2005; Tsukada et al., 2005; Moores et al., 2006; Yap et al., 2012; Fu et al., 2013). Another, p27^{kip1} (Cdkn1b – Mouse Genome Informatics) controls microtubule and actin cytoskeletal organization (Kawauchi et al., 2006; Godin et al., 2012). As previously reported (Tanaka et al., 2004b; Kawauchi et al., 2006), Cdk5 knockdown decreased the phosphorylation of Dcx and p27^{kip1} at Ser297 and Ser10, respectively, and total protein levels of p27^{kip1} (supplementary material Fig. S2D,E).

Because Cdk5-mediated phosphorylation is known to negatively regulate Dcx, we overexpressed Dcx. Overexpression of wt-Dcx decreased the ratio of cells with dilation and with elongated nucleus in the locomoting neurons in cortical slices and fixed cortical sections (supplementary material Fig. S9). Importantly, knockdown of Dcx partially rescued the defects in dilation formation and nuclear elongation in the Cdk5-knockdown locomoting neurons (supplementary material Fig. S9).

Knockdown of Dcx alone also disturbed dilation formation and nuclear elongation (Fig. 8), suggesting that proper regulation of Dcx activity is important for the locomotion mode of migration. These defects were rescued by the co-expression of wt-Dcx (Fig. 8), and therefore not due to off-targeting effects. In our experimental conditions, the majority of Dcx-knockdown neurons

Development (2014) 141, 3540-3550 doi:10.1242/dev.111294

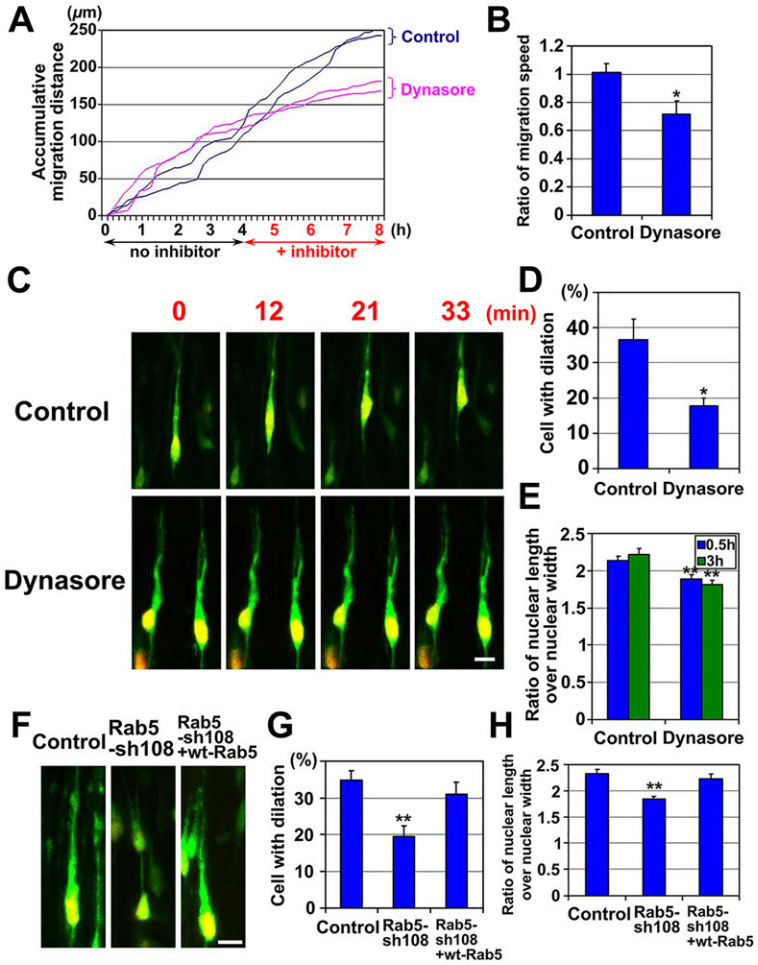

Fig. 6. Endocytic pathways are required for cytoplasmic dilation formation. (A) Accumulative migration distances of two control cells (blue lines) or two dynasore-treated cells (magenta lines). During the first 4 h (shown in black), there was no inhibitor. At 4 h, dynasore or solvent (control) was added. (B) Migration speeds of locomoting neurons were measured in cortical slices before and after treatment with the indicated inhibitors. The ratios of their migration speeds after inhibitor treatment to before inhibitor treatment were calculated. Control and dynasore: *n*=10 cells (four slices). (C) Time-lapse observation of locomoting neurons in cortical slices with or without dynasore (40 μM). (D) Ratios of cells with a cytoplasmic dilation at 3 h after inhibitor treatment. Control: *n*=40 cells (four slices); dynasore, *n*=49 cells (four slices). (E) Ratios of length to width of nuclei in locomoting neurons at 0.5 or 3 h after inhibitor treatment. Control and dynasore, *n*=36 cells (three slices). (F) Representative images of control or Rab5-knockdown or Rab5-knockdown-rescued locomoting neurons. Co-electroporated EGFP and NLS-DsRed signals are shown. (G) Ratio of cells with a cytoplasmic dilation. Control, *n*=44 cells (four slices); Rab5-sh108, *n*=61 cells (five slices); Rab5-sh108+wt-Rab5, *n*=58 cells (four slices). (H) Ratios of length to width of nuclei in Rab5-knockdown locomoting neurons. Control, Rab5-sh108 and Rab5-sh108+wt-Rab5, *n*=30 cells (three slices). Data are mean±s.e.m. Significance of differences was determined using Welch's *t*-test (B) or Student's *t*-test (D,E,G,H). **P*<0.05, ***P*<0.01. Scale bars: 20 μm in C; 10 μm in F.

entered the cortical plate, but their migration speeds were decreased (supplementary material Fig. S10), which is consistent with previous observations in Dcx-knockout mice (Pramparo et al., 2010).

Knockdown of $p27^{kip1}$ suppressed dilation formation and nuclear elongation in the locomoting neurons in cortical slices and fixed cortical sections; these defects were rescued by the co-expression of human wt-$p27^{kip1}$, suggesting that $p27^{kip1}$ also plays some roles in the locomotion mode of neuronal migration (Fig. 8). However, overexpression of a Ser10-phospho-mimic mutant of $p27^{kip1}$ (p27-S10D) did not rescue the Cdk5-knockdown phenotypes, probably because Cdk5 regulates many downstream events (supplementary material Figs S9 and S11).

DISCUSSION

Neuronal migration is a fundamental cellular event towards constructing a functional brain, and defects in neuronal migration result in various neurological disorders, including lissencephaly (Gleeson and Walsh, 2000; Kawauchi and Hoshino, 2008). In the developing cerebral cortex, the majority of migrating neurons

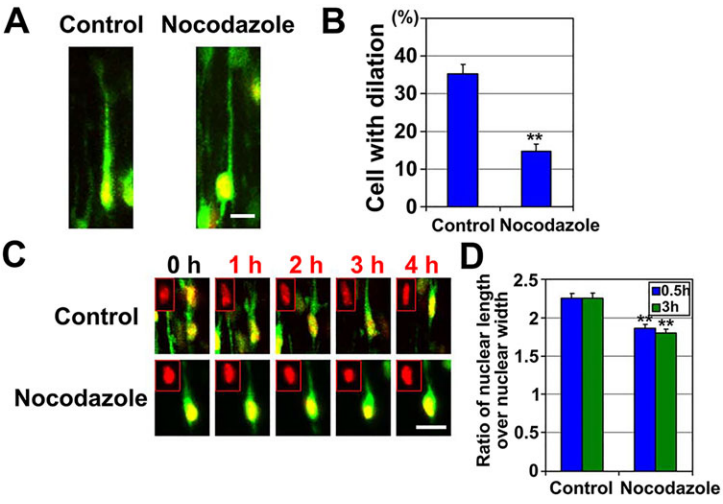

Fig. 7. Microtubule organization is required for cytoplasmic dilation formation. (A) Representative images of the locomoting neurons in cortical slices with or without nocodazole (100 nM). (B) Ratios of cells with a cytoplasmic dilation 3 h after inhibitor treatment. Control, *n*=39 cells (four slices); nocodazole, *n*=60 cells (six slices). (C) Time-lapse observation of locomoting neurons in cortical slices with or without nocodazole (100 nM). Cortical slices were treated with inhibitor just after 0 h. The insets show nuclear morphologies, visualized by NLS-DsRed-mediated fluorescence. (D) Ratios of length to width of nuclei in locomoting neurons at 0.5 or 3 h after inhibitor treatment. Control, *n*=36 cells (three slices); nocodazole, *n*=48 cells (six slices). Data are mean± s.e.m. Significance of differences was determined using Student's *t*-test. ***P*<0.01. Scale bars: 10 μm in A; 20 μm in C.

Development (2014) 141, 3540-3550 doi:10.1242/dev.111294

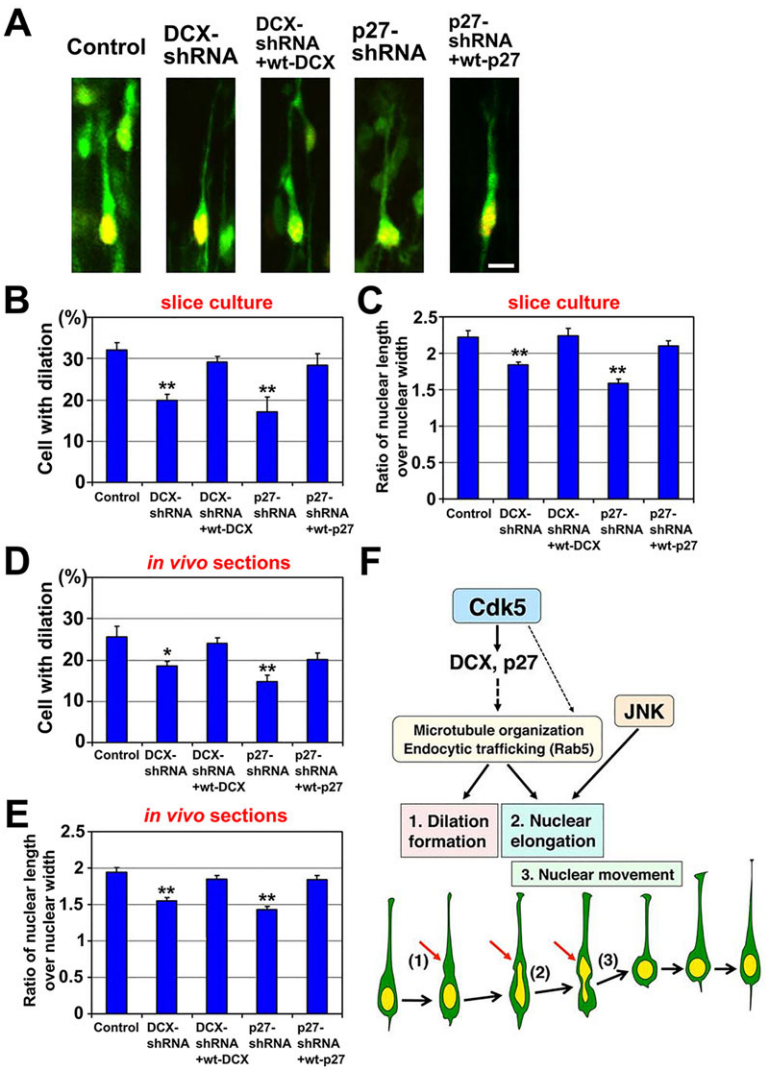

Fig. 8. Dcx and p27^{kip1} regulate dilation formation and nuclear elongation. (A) Representative images of control, Dcx-knockdown, Dcx-knockdown-rescued, p27^{kip1}-knockdown or p27^{kip1}-knockdown-rescued locomoting neurons. (B,D) Ratios of cells with a cytoplasmic dilation in cortical slice cultures (B) or *in vivo* cortical sections (D). Control, *n*=47 cells (four slices); Dcx-shRNA, *n*=60 cells (five slices); Dcx-shRNA+wt-Dcx, *n*=44 cells (four slices); p27-shRNA, *n*=49 cells (five slices); p27-shRNA+wt-p27^{kip1}, *n*=40 cells (four slices) in B. Control, *n*=67 cells (six sections); Dcx-shRNA, *n*=82 cells (five sections); Dcx-shRNA+wt-Dcx, *n*=37 cells (three sections); p27-shRNA, *n*=54 cells (six sections); p27-shRNA+wt-p27^{kip1}, *n*=44 cells (six sections) in D. (C,E) Ratios of length to width of nuclei in locomoting neurons in cortical slice cultures (C) or *in vivo* cortical sections (E). Control, Dcx-shRNA, p27-shRNA and p27-shRNA+wt-p27^{kip1}, *n*=30 cells (three slices); Dcx-shRNA+wt-Dcx, *n*=20 cells (two slices) in C. Control, Dcx-shRNA, Dcx-shRNA+wt-Dcx, p27-shRNA and p27-shRNA+wt-p27^{kip1}, *n*=30 cells (three sections) in E. (F) Schematic of the molecular mechanisms of dilation formation and nuclear elongation. Migrating neurons exhibit unique morphological changes: they form a cytoplasmic dilation (1), followed by nuclear elongation (2) and forward movement (3). Cdk5 and its substrates Dcx and p27^{kip1} regulate dilation formation and nuclear elongation, whereas Jnk controls nuclear elongation, but not dilation formation. Cdk5 controls Rab5-dependent endocytic trafficking and microtubule organization, both of which are also required for dilation formation and nuclear elongation. Red arrows indicate dilation. Data are mean±s.e.m. Significance of differences was determined using Student's *t*-test. **P*<0.05, ***P*<0.01. Scale bar: 10 µm.

exhibit the locomoting morphology. They extend a leading process and form a cytoplasmic dilation at the proximal region of the leading process. The cytoplasmic dilation is a migrating neuron-specific structure and thought to be essential for the forward movement (Bellion et al., 2005; Schaar and McConnell, 2005). Therefore, it determines the character of the unique migration pattern of neurons. In this study, we show that Cdk5, a molecule predominantly activated in neurons, is important for the neuron-specific migrating features: the formation of the cytoplasmic dilation and nuclear elongation.

Cdk5 is known to control dynein-dependent motor activity mainly through the regulation of the Ndel1-Lis1 complex (Ayala et al., 2007). However, knockdown of dynein heavy chain or Lis1 does not affect the cytoplasmic dilation formation, although inhibition of either protein perturbs nuclear forward movement (Tsai et al., 2007), suggesting that another cellular event is involved in the Cdk5-mediated dilation formation. Although Dcx and Lis1, causative gene products of lissencephaly, share some common functions in the dynein-mediated regulation of centrosome positioning (Tanaka et al., 2004a), Dcx plays other roles in microtubule polymerization and endocytic trafficking (Francis et al., 1999; Gleeson et al., 1999; Friocourt et al., 2005; Moores et al., 2006; Yap et al., 2012), which are shown here to regulate dilation formation. These dynein-independent functions of Dcx may have important roles in dilation formation. It is consistent with a previous report that deficiency of Diap1 and Diap3 (previously mDia1 and mDia3) disturbs the centrosomal positioning, but not swelling/dilation formation in cortical interneurons (Shinohara et al., 2012), suggesting that the regulation of dynein activity and its mediated centrosomal positioning may be distinct from dilation formation.

In addition to Dcx, p27^{kip1} has been shown to regulate dilation formation. Interestingly, suppression of p27^{kip1} in cortical interneurons promotes swelling/dilation formation (Godin et al., 2012), suggesting that regulation of swelling/dilation formation in future excitatory and inhibitory neurons require different mechanisms. The distance between the swelling/dilation and nucleus of interneurons is longer than that of excitatory neurons (Bellion et al., 2005). Interestingly, knockdown of p27^{kip1} slightly increased the 'interneuron-type' of swelling/dilation (data not shown). Conversely, the deficiency of Diap1 and Diap3, which are involved in the migration of cortical interneurons but not of excitatory projection neurons, results in less separation of the cell soma from the swelling/dilation (Shinohara et al., 2012). Thus, p27^{kip1} and Diap proteins might regulate the neuronal subtype-specific migration pattern.

A recent report indicates that Rac1 and POSH, a Rac1 interacting protein, are required for dilation formation (Yang et al., 2012). The relationship between Cdk5 and Rac1 activity has been reported (Nikolic et al., 1998; Xin et al., 2004), and Posh contains several

Development (2014) 141, 3540-3550 doi:10.1242/dev.111294

proline-directed Ser/Thr residues, which are potential phosphorylation targets of Cdk5. Therefore, Cdk5 might control the formation of a cytoplasmic dilation in cooperation with Rac1 and POSH.

Nuclear elongation during the locomotion mode of neuronal migration is a process by which the nucleus enters the dilation, implicating nuclear elongation as an important step for the forward movement (Bellion et al., 2005; Schaar and McConnell, 2005). Interestingly, unlike cytoplasmic dilation formation, Jnk and Cdk5 are required for nuclear elongation and forward movement. The decrease of migration speed in the Jnk1-knockdown neurons is consistent with that observed in mice with knockouts of Jnk upstream kinases (*Mkk4*, *Mkk7*, *Dlk* or *Mekk4*) or electroporated with dominant-negative Jnk1 (Kawauchi et al., 2003; Sarkisian et al., 2006; Wang et al., 2007; Yamasaki et al., 2011). Both Jnk and Cdk5 are known to control microtubule stability and organization (Kawauchi et al., 2003, 2005; Gdalyahu et al., 2004), implying that Jnk and Cdk5 may cooperatively control nuclear elongation via microtubule regulation. Interestingly, nuclear Jnk has a role in neuronal migration (Westerlund et al., 2011), implying that Jnk might directly regulate nuclear morphological changes.

The relationship between Cdk5 and endocytic pathways is still controversial. Endocytic pathways consist of various trafficking pathways that originate from endocytosis, such as endocytosis, recycling and lysosomal degradation pathways (Stenmark, 2009). At the presynapse, Cdk5 negatively regulates endocytosis via phosphorylation of dynamin 1 and amphiphysin 1 (Floyd et al., 2001; Tomizawa et al., 2003), although inhibition of Cdk5 is reported to disturb the phosphorylation/dephosphorylation cycle of dynamin 1 and amphiphysin 1, resulting in a defect in endocytosis at the presynapse (Tan et al., 2003; Evans and Cousin, 2007). By contrast, Cdk5 promotes the endocytosis of NMDA receptors at postsynaptic sites (Zhang et al., 2008). Cdk5 also regulates the N-cadherin-mediated cell adhesion (Kwon et al., 2000) and a Rab11-dependent recycling pathway (Takano et al., 2012), both of which are important for neuronal migration (Kawauchi et al., 2010). Therefore, whether the total output of Cdk5 function promotes or suppresses endocytic pathways may be dependent on cell type or on local environment. Our data show that Cdk5 inhibition disturbs the trafficking of transferrin at Rab5-positive early endosomes, suggesting that Cdk5 coordinates the early steps of endocytic trafficking in embryonic cortical neurons. Alternatively, Cdk5 may indirectly control endocytic pathways via the regulation of microtubule organization.

We have previously reported that Rab5-dependent endocytosis is required for several steps of neuronal migration, including the radial fiber-dependent locomotion mode (Kawauchi et al., 2010; Shikanai et al., 2011). However, in a series of these experiments, Rab5-shRNAs were expressed prior to the transition to the locomotion mode. In this study, our *ex vivo* chemical inhibitor experiments clearly show that blocking endocytosis disturbs the locomotion mode of neuronal migration. Together with our previous results (Kawauchi et al., 2010) and a report from Susan McConnell's group (Shieh et al., 2011), the present study provides a model in which, under the control of Cdk5, N-cadherin is internalized at the cytoplasmic dilation in a clathrin- and Rab5-dependent manner and recycled back to the plasma membrane, a cycle that is essential for the radial fiber-dependent locomotion mode of neuronal migration.

MATERIALS AND METHODS

Plasmids

Plasmids were prepared using the EndoFree plasmid purification kit (Qiagen). EGFP-wt-Rab5 (human) (Rosenfeld et al., 2001), mouse wt-Dcx without 3′UTR, EYFP-Golgi (Clontech) and DsRed-monomer-Golgi (Clontech) cDNAs were inserted into pCAG=MCS2 (Kawauchi et al., 2005) to generate CAG=EGFP-wt-Rab5, CAG=wt-Dcx, CAG=EYFP-Golgi and CAG=DsRed-monomer-Golgi. CAG=EGFP, CAG=nuclear localizing signal (NLS)-fused DsRed, CAG=EGFP-actin, CAG=wt-Cdk5 (human), CAG=wt-Jnk1 (human), CAG=wt-Rab5 (human), CAG=p27-S10D (human), CAG=wt-p27 (human), Cdk5-sh250 (shCK5B), Rab5-sh108 and p27-shRNA (sh27A) have been described previously (Kawauchi et al., 2003, 2006, 2010; Nishimura et al., 2010). To construct shRNA-expressing vectors, oligonucleotides targeting the Jnk1-coding sequence (Jnk1-sh788: 5′-GGCCTAAATACGCTGGATA-3′) or a control scrambled sequence (sh-scr2: 5′-CGTCGGATAATACTAATCT-3′), and their complementary sequences were inserted into the mU6pro vector (Yu et al., 2002). All contain a nine-base hairpin loop sequence (5′-TTCAAGAGA-3′). These sequences were designed based on information from shRNA sequence analyses (B-Bridge International). Dcx-shRNA targeting the Dcx 3′UTR sequence (5′-GCTCAAGTGACCAACAAGGCTAT-3′) was constructed as described previously (Ramos et al., 2006).

Antibodies and chemical regents

Primary antibodies used in this study were anti-Jnk (Cell Signaling, 9252, 1/1000), anti-Cdk5 (Santa Cruz, sc-6247, 1/100), anti-β-tubulin (Sigma, T5201, 1/5000 for immunoblot, 1/400 for immunocytochemistry), anti-S732-phosphorylated FAK (Sigma, F7803, 1/500), anti-FAK (Santa Cruz, sc-932, 1/500), anti-p35 (Santa Cruz, sc-820, 1/500), anti-S10-phosphorylated p27 (Zymed, 34-6300, 1/100), anti-p27 (BD Biosciences, 610241, 1/1000), anti-S297-phosphorylated Dcx (Cell Signaling, 4605, 1/100), anti-Dcx (Abcam, ab18723, 1/500), anti-EGFP (Molecular Probes, A6455, 1/1500), anti-Glu-tubulin (Chemicon, AB3201, 1/100), anti-p115 (BD Biosciences, 612260, 1/100) and anti-GM130 (Cell Signaling, 2296, 1/100). Roscovitine, nocodazole, cytochalasin D and latrunculin B were purchased from Sigma, bisindolylmaleimide I (BIM) and rottlerin from Calbiochem, dynasore from Santa Cruz, SP600125 from BIOMOL, 4′,6-diamidino-2-phenylindole dihydrochloride solution (DAPI) from Wako and Alexa594-conjugated transferrin from Molecular Probes.

In utero electroporation and slice culture of embryonic cerebral cortex

Pregnant ICR mice were obtained from SLC Japan. Animals were handled in accordance with guidelines established by Keio University, Aichi Human Service Center and NCNP. *In utero* electroporation was performed on E14 embryos, as described previously (Kawauchi et al., 2003). Cortical slice culture was performed as described previously (Nishimura et al., 2010). Briefly, the electroporated brains at E16 were cut into 300 μm coronal slices with a microtome (Leica), and cortical slices were cultured under confocal laser scanning time-lapse microscopy, FV1000 (Olympus) or TCL-SP2 (Leica). The following inhibitors were added to culture media; control DMSO (0.1%), roscovitine (100 μM), rottlerin (5 μM), SP600125 (50 μM), dynasore (40 μM), nocodazole (100 nM), cytochalasin D (10 μM) and latrunculin B (10 μM).

Primary culture, transfection, immunoblot analysis and immunohistochemistry

Primary culture of embryonic cerebral cortices, transfection and immunoblot analysis were performed as described previously (Kawauchi et al., 2003, 2006, 2010). For immunohistochemistry, frozen cortical sections were treated with HistoVT-One (Nacalai) for 20 min at 70°C, and other steps were performed as described previously (Kawauchi et al., 2010).

Transferrin uptake assay and immunocytochemistry

E15 cerebral cortices were dissociated and cultured for 2 days. Primary cultured neurons were incubated in Opti-MEM media (Invitrogen) for 30 min at 37°C and treated with 20 μg/ml Alexa594-conjugated transferrin in Opti-MEM media. After incubation for 5-15 min on ice, neurons were incubated for 10 or 30 min at 37°C.

For immunocytochemistry, cortical neurons were fixed with 4% PFA in PBS for 20 min, permeabilized with 10% goat serum in PBS (GS-PBS)

Development (2014) 141, 3540-3550 doi:10.1242/dev.111294

containing 0.15% Triton X-100 for 5 min and blocked with GS-PBS for 30 min at room temperature. Subsequently, the cultured neurons were incubated with diluted primary antibodies in GS-PBT (GS-PBS containing 0.1% Tween20) at 4°C overnight. After three washes in PBS, neurons were treated with Alexa488- or Alexa555-conjugated secondary antibodies (Molecular Probes) diluted in PBS for 60 min at room temperature, followed by three washes in PBS. Fluorescent images were obtained by TCL-SL or TCL-SP5 laser scanning confocal microscopy (Leica).

Quantitative and statistical analyses

Migration speed was analyzed by DippMotion 2D software (Ditect). Dilation was defined as a swollen leading process (more than one-third of the nuclear diameter) at the proximal region (5 µm above the pial edge of the nucleus) with a narrowing between the swollen region and nucleus. Dilation area was defined as the maximum area of leading processes in 10 µm distances from the cell soma during 10 h time-lapse observations. Nuclear sphericity was analyzed using Imaris software (Bitplane). Sphericity was defined by Wadell in 1935 (Wadell, 1935) as a measure criterion of 'how spherical an object is' and calculated as the ratio of the surface area of a sphere with the same volume as the given particle to the surface area of the particle.

Data are presented as mean±s.e.m. Statistical significance was calculated using two-tailed Student's *t*-test or Welch's *t*-test. $P<0.05$ was considered statistically significant.

Acknowledgements

We thank Drs Brian J. Knoll (University of Houston), Jun-ichi Miyazaki (Osaka University) and David L. Turner (University of Michigan) for providing plasmids. The authors also thank Drs Ruth T. Yu (Salk Institute), Michisuke Yuzaki (Keio University) and Satoshi Miyashita (NCNP) for proofreading of the manuscript, providing the experimental environments and supporting time-lapse experiments, respectively.

Competing interests

The authors declare no competing financial interests.

Author contributions

T.K. conceived and directed the project, performed primary culture experiments and analyzed the data. Y.V.N. performed all of the slice culture experiments and analyzed the data. M.S. performed primary culture experiments. K.N., K.-i.N., T.K., M.H., Y.-i.N., T.O. and K.-i.M. administered the experimental environments. T.K. wrote the paper with the help of Y.V.N.

Funding

This work was supported by Grants-in-Aid from the Ministry of Education, Culture, Sports, Science and Technology, Japan [26290015 to T.K., 26110718 to T.K., 25870900 to Y.V.N., 22111004 to K.N. and 24390271 to K.-i.N.), and by grants from the JST PRESTO program (to T.K.) and the Strategic Research Program for Brain Science (Understanding of molecular and environmental bases for brain health, to K.N.).

Supplementary material

Supplementary material available online at
http://dev.biologists.org/lookup/suppl/doi:10.1242/dev.111294/-/DC1

References

Asada, A., Saito, T. and Hisanaga, S.-I. (2012). Phosphorylation of p35 and p39 by Cdk5 determines the subcellular location of the holokinase in a phosphorylation-site-specific manner. *J. Cell Sci.* **125**, 3421-3429.

Ayala, R., Shu, T. and Tsai, L.-H. (2007). Trekking across the brain: the journey of neuronal migration. *Cell* **128**, 29-43.

Bain, J., McLauchlan, H., Elliott, M. and Cohen, P. (2003). The specificities of protein kinase inhibitors: an update. *Biochem. J.* **371**, 199-204.

Bain, J., Plater, L., Elliott, M., Shpiro, N., Hastie, C. J., McLauchlan, H., Klevernic, I., Arthur, J. S., Alessi, D. R. and Cohen, P. (2007). The selectivity of protein kinase inhibitors: a further update. *Biochem. J.* **408**, 297-315.

Bellion, A., Baudoin, J.-P., Alvarez, C., Bornens, M. and Métin, C. (2005). Nucleokinesis in tangentially migrating neurons comprises two alternating phases: forward migration of the Golgi/centrosome associated with centrosome splitting and myosin contraction at the rear. *J. Neurosci.* **25**, 5691-5699.

Edmondson, J. C. and Hatten, M. E. (1987). Glial-guided granule neuron migration in vitro: a high-resolution time-lapse video microscopic study. *J. Neurosci.* **7**, 1928-1934.

Evans, G. J. O. and Cousin, M. A. (2007). Activity-dependent control of slow synaptic vesicle endocytosis by cyclin-dependent kinase 5. *J. Neurosci.* **27**, 401-411.

Floyd, S. R., Porro, E. B., Slepnev, V. I., Ochoa, G.-C., Tsai, L.-H. and De Camilli, P. (2001). Amphiphysin 1 binds the cyclin-dependent kinase (cdk) 5 regulatory subunit p35 and is phosphorylated by cdk5 and cdc2. *J. Biol. Chem.* **276**, 8104-8110.

Francis, F., Koulakoff, A., Boucher, D., Chafey, P., Schaar, B., Vinet, M.-C., Friocourt, G., McDonnell, N., Reiner, O., Kahn, A. et al. (1999). Doublecortin is a developmentally regulated, microtubule-associated protein expressed in migrating and differentiating neurons. *Neuron* **23**, 247-256.

Friocourt, G., Kappeler, C., Saillour, Y., Fauchereau, F., Rodriguez, M. S., Bahi, N., Vinet, M.-C., Chafey, P., Poirier, K., Taya, S. et al. (2005). Doublecortin interacts with the ubiquitin protease DFFRX, which associates with microtubules in neuronal processes. *Mol. Cell. Neurosci.* **28**, 153-164.

Fu, X., Brown, K. J., Yap, C. C., Winckler, B., Jaiswal, J. K. and Liu, J. S. (2013). Doublecortin (Dcx) family proteins regulate filamentous actin structure in developing neurons. *J. Neurosci.* **33**, 709-721.

Gdalyahu, A., Ghosh, I., Levy, T., Sapir, T., Sapoznik, S., Fishler, Y., Azoulai, D. and Reiner, O. (2004). DCX, a new mediator of the JNK pathway. *EMBO J.* **23**, 823-832.

Gleeson, J. G. and Walsh, C. A. (2000). Neuronal migration disorders: from genetic diseases to developmental mechanisms. *Trends Neurosci.* **23**, 352-359.

Gleeson, J. G., Lin, P. T., Flanagan, L. A. and Walsh, C. A. (1999). Doublecortin is a microtubule-associated protein and is expressed widely by migrating neurons. *Neuron* **23**, 257-271.

Godin, J. D., Thomas, N., Laguesse, S., Malinouskaya, L., Close, P., Malaise, O., Purnelle, A., Raineteau, O., Campbell, K., Fero, M. et al. (2012). p27(Kip1) is a microtubule-associated protein that promotes microtubule polymerization during neuron migration. *Dev. Cell* **23**, 729-744.

Govek, E.-E., Hatten, M. E. and Van Aelst, L. (2011). The role of Rho GTPase proteins in CNS neuronal migration. *Dev. Neurobiol.* **71**, 528-553.

Gschwendt, M., Muller, H. J., Kielbassa, K., Zang, R., Kittstein, W., Rincke, G. and Marks, F. (1994). Rottlerin, a novel protein kinase inhibitor. *Biochem. Biophys. Res. Commun.* **199**, 93-98.

Hisanaga, S.-I. and Saito, T. (2003). The regulation of cyclin-dependent kinase 5 activity through the metabolism of p35 or p39 Cdk5 activator. *Neurosignals* **12**, 221-229.

Kang, J.-W., Park, Y. S., Kim, M. S., Lee, D. H., Bak, Y., Ham, S. Y., Park, S. H., Hong, J. T. and Yoon, D.-Y. (2013). Interleukin (IL)-32beta-mediated CCAAT/enhancer-binding protein alpha (C/EBPalpha) phosphorylation by protein kinase Cdelta (PKCdelta) abrogates the inhibitory effect of C/EBPalpha on IL-10 production. *J. Biol. Chem.* **288**, 23650-23658.

Kawauchi, T. (2012). Cell adhesion and its endocytic regulation in cell migration during neural development and cancer metastasis. *Int. J. Mol. Sci.* **13**, 4564-4590.

Kawauchi, T. (2014). Cdk5 regulates multiple cellular events in neural development, function and disease. *Dev. Growth Differ.* **56**, 335-348.

Kawauchi, T. and Hoshino, M. (2008). Molecular pathways regulating cytoskeletal organization and morphological changes in migrating neurons. *Dev. Neurosci.* **30**, 36-46.

Kawauchi, T., Chihama, K., Nabeshima, Y.-I. and Hoshino, M. (2003). The in vivo roles of STEF/Tiam1, Rac1 and JNK in cortical neuronal migration. *EMBO J.* **22**, 4190-4201.

Kawauchi, T., Chihama, K., Nishimura, Y. V., Nabeshima, Y.-I. and Hoshino, M. (2005). MAP1B phosphorylation is differentially regulated by Cdk5/p35, Cdk5/p25, and JNK. *Biochem. Biophys. Res. Commun.* **331**, 50-55.

Kawauchi, T., Chihama, K., Nabeshima, Y.-I. and Hoshino, M. (2006). Cdk5 phosphorylates and stabilizes p27kip1 contributing to actin organization and cortical neuronal migration. *Nat. Cell Biol.* **8**, 17-26.

Kawauchi, T., Sekine, K., Shikanai, M., Chihama, K., Tomita, K., Kubo, K.-I., Nakajima, K., Nabeshima, Y.-I. and Hoshino, M. (2010). Rab GTPases-dependent endocytic pathways regulate neuronal migration and maturation through N-cadherin trafficking. *Neuron* **67**, 588-602.

Kawauchi, T., Shikanai, M. and Kosodo, Y. (2013). Extra-cell cycle regulatory functions of cyclin-dependent kinases (CDK) and CDK inhibitor proteins contribute to brain development and neurological disorders. *Genes Cells***18**, 176-194.

Kwon, Y. T., Gupta, A., Zhou, Y., Nikolic, M. and Tsai, L.-H. (2000). Regulation of N-cadherin-mediated adhesion by the p35-Cdk5 kinase. *Curr. Biol.* **10**, 363-372.

Macia, E., Ehrlich, M., Massol, R., Boucrot, E., Brunner, C. and Kirchhausen, T. (2006). Dynasore, a cell-permeable inhibitor of dynamin. *Dev. Cell.* **10**, 839-850.

Meijer, L., Borgne, A., Mulner, O., Chong, J. P. J., Blow, J. J., Inagaki, N., Inagaki, M., Delcros, J.-G. and Moulinoux, J.-P. (1997). Biochemical and cellular effects of roscovitine, a potent and selective inhibitor of the cyclin-dependent kinases cdc2, cdk2 and cdk5. *Eur. J. Biochem.* **243**, 527-536.

Moores, C. A., Perderiset, M., Kappeler, C., Kain, S., Drummond, D., Perkins, S. J., Chelly, J., Cross, R., Houdusse, A. and Francis, F. (2006). Distinct roles of doublecortin modulating the microtubule cytoskeleton. *EMBO J.* **25**, 4448-4457.

Nadarajah, B. and Parnavelas, J. G. (2002). Modes of neuronal migration in the developing cerebral cortex. *Nat. Rev. Neurosci.* **3**, 423-432.

Niethammer, M., Smith, D. S., Ayala, R., Peng, J., Ko, J., Lee, M.-S., Morabito, M. and Tsai, L.-H. (2000). NUDEL is a novel Cdk5 substrate that associates with LIS1 and cytoplasmic dynein. *Neuron* **28**, 697-711.
Nikolic, M., Chou, M. M., Lu, W., Mayer, B. J. and Tsai, L.-H. (1998). The p35/Cdk5 kinase is a neuron-specific Rac effector that inhibits Pak1 activity. *Nature* **395**, 194-198.
Nishimura, Y. V., Sekine, K., Chihama, K., Nakajima, K., Hoshino, M., Nabeshima, Y.-I. and Kawauchi, T. (2010). Dissecting the factors involved in the locomotion mode of neuronal migration in the developing cerebral cortex. *J. Biol. Chem.* **285**, 5878-5887.
Nobes, C. D. and Hall, A. (1995). Rho, rac, and cdc42 GTPases regulate the assembly of multimolecular focal complexes associated with actin stress fibers, lamellipodia, and filopodia. *Cell* **81**, 53-62.
Ohshima, T., Hirasawa, M., Tabata, H., Mutoh, T., Adachi, T., Suzuki, H., Saruta, K., Iwasato, T., Itohara, S., Hashimoto, M. et al. (2007). Cdk5 is required for multipolar-to-bipolar transition during radial neuronal migration and proper dendrite development of pyramidal neurons in the cerebral cortex. *Development* **134**, 2273-2282.
Pramparo, T., Youn, Y. H., Yingling, J., Hirotsune, S. and Wynshaw-Boris, A. (2010). Novel embryonic neuronal migration and proliferation defects in Dcx mutant mice are exacerbated by Lis1 reduction. *J. Neurosci.* **30**, 3002-3012.
Rakic, P. (1972). Mode of cell migration to the superficial layers of fetal monkey neocortex. *J. Comp. Neurol.* **145**, 61-83.
Ramos, R. L., Bai, J. and LoTurco, J. J. (2006). Heterotopia formation in rat but not mouse neocortex after RNA interference knockdown of DCX. *Cereb. Cortex.* **16**, 1323-1331.
Rosenfeld, J. L., Moore, R. H., Zimmer, K. P., Alpizar-Foster, E., Dai, W., Zarka, M. N. and Knoll, B. J. (2001). Lysosome proteins are redistributed during expression of a GTP-hydrolysis-defective rab5a. *J. Cell Sci.* **114**, 4499-4508.
Sarkisian, M. R., Bartley, C. M., Chi, H., Nakamura, F., Hashimoto-Torii, K., Torii, M., Flavell, R. A. and Rakic, P. (2006). MEKK4 signaling regulates filamin expression and neuronal migration. *Neuron* **52**, 789-801.
Schaar, B. T. and McConnell, S. K. (2005). Cytoskeletal coordination during neuronal migration. *Proc. Natl. Acad. Sci. USA* **102**, 13652-13657.
Shieh, J. C., Schaar, B. T., Srinivasan, K., Brodsky, F. M. and McConnell, S. K. (2011). Endocytosis regulates cell soma translocation and the distribution of adhesion proteins in migrating neurons. *PLoS ONE* **6**, e17802.
Shikanai, M., Nakajima, K. and Kawauchi, T. (2011). N-cadherin regulates radial glial fiber-dependent migration of cortical locomoting neurons. *Commun. Integr. Biol.* **4**, 326-330.
Shinohara, R., Thumkeo, D., Kamijo, H., Kaneko, N., Sawamoto, K., Watanabe, K., Takebayashi, H., Kiyonari, H., Ishizaki, T., Furuyashiki, T. et al. (2012). A role for mDia, a Rho-regulated actin nucleator, in tangential migration of interneuron precursors. *Nat. Neurosci.* **15**, 373-380, S371-372.
Solecki, D. J., Trivedi, N., Govek, E.-E., Kerekes, R. A., Gleason, S. S. and Hatten, M. E. (2009). Myosin II motors and F-actin dynamics drive the coordinated movement of the centrosome and soma during CNS glial-guided neuronal migration. *Neuron* **63**, 63-80.
Stenmark, H. (2009). Rab GTPases as coordinators of vesicle traffic. *Nat. Rev. Mol. Cell Biol.* **10**, 513-525.
Takano, T., Tomomura, M., Yoshioka, N., Tsutsumi, K., Terasawa, Y., Saito, T., Kawano, H., Kamiguchi, H., Fukuda, M. and Hisanaga, S.-I. (2012). LMTK1/AATYK1 is a novel regulator of axonal outgrowth that acts via Rab11 in a Cdk5-dependent manner. *J. Neurosci.* **32**, 6587-6599.
Tan, T. C., Valova, V. A., Malladi, C. S., Graham, M. E., Berven, L. A., Jupp, O. J., Hansra, G., McClure, S. J., Sarcevic, B., Boadle, R. A. et al. (2003). Cdk5 is essential for synaptic vesicle endocytosis. *Nat. Cell Biol.* **5**, 701-710.
Tanaka, T., Serneo, F. F., Higgins, C., Gambello, M. J., Wynshaw-Boris, A. and Gleeson, J. G. (2004a). Lis1 and doublecortin function with dynein to mediate coupling of the nucleus to the centrosome in neuronal migration. *J. Cell Biol.* **165**, 709-721.
Tanaka, T., Serneo, F. F., Tseng, H.-C., Kulkarni, A. B., Tsai, L.-H. and Gleeson, J. G. (2004b). Cdk5 phosphorylation of doublecortin ser297 regulates its effect on neuronal migration. *Neuron* **41**, 215-227.
Tomizawa, K., Sunada, S., Lu, Y.-F., Oda, Y., Kinuta, M., Ohshima, T., Saito, T., Wei, F.-Y., Matsushita, M., Li, S.-T. et al. (2003). Cophosphorylation of amphiphysin I and dynamin I by Cdk5 regulates clathrin-mediated endocytosis of synaptic vesicles. *J. Cell Biol.* **163**, 813-824.
Trischler, M., Stoorvogel, W. and Ullrich, O. (1999). Biochemical analysis of distinct Rab5- and Rab11-positive endosomes along the transferrin pathway. *J. Cell Sci.* **112**, 4773-4783.
Tsai, L. H., Takahashi, T., Caviness, V. S., Jr and Harlow, E. (1993). Activity and expression pattern of cyclin-dependent kinase 5 in the embryonic mouse nervous system. *Development* **119**, 1029-1040.
Tsai, J.-W., Bremner, K. H. and Vallee, R. B. (2007). Dual subcellular roles for LIS1 and dynein in radial neuronal migration in live brain tissue. *Nat. Neurosci.* **10**, 970-979.
Tsukada, M., Prokscha, A., Ungewickell, E. and Eichele, G. (2005). Doublecortin association with actin filaments is regulated by neurabin II. *J. Biol. Chem.* **280**, 11361-11368.
Ullrich, O., Reinsch, S., Urbe, S., Zerial, M. and Parton, R. G. (1996). Rab11 regulates recycling through the pericentriolar recycling endosome. *J. Cell Biol.* **135**, 913-924.
Wadell, H. (1935). Volume, shape, and roundness of quartz particles. *J. Geol.* **43**, 250-280.
Wang, X., Nadarajah, B., Robinson, A. C., McColl, B. W., Jin, J.-W., Dajas-Bailador, F., Boot-Handford, R. P. and Tournier, C. (2007). Targeted deletion of the mitogen-activated protein kinase kinase 4 gene in the nervous system causes severe brain developmental defects and premature death. *Mol. Cell. Biol.* **27**, 7935-7946.
Westerlund, N., Zdrojewska, J., Padzik, A., Komulainen, E., Björkblom, B., Rannikko, E., Tararuk, T., Garcia-Frigola, C., Sandholm, J., Nguyen, L. et al. (2011). Phosphorylation of SCG10/stathmin-2 determines multipolar stage exit and neuronal migration rate. *Nat. Neurosci.* **14**, 305-313.
Wilson, P. M., Fryer, R. H., Fang, Y. and Hatten, M. E. (2010). Astn2, a novel member of the astrotactin gene family, regulates the trafficking of ASTN1 during glial-guided neuronal migration. *J. Neurosci.* **30**, 8529-8540.
Xie, Z., Sanada, K., Samuels, B. A., Shih, H. and Tsai, L.-H. (2003). Serine 732 phosphorylation of FAK by Cdk5 is important for microtubule organization, nuclear movement, and neuronal migration. *Cell* **114**, 469-482.
Xin, X., Ferraro, F., Back, N., Eipper, B. A. and Mains, R. E. (2004). Cdk5 and Trio modulate endocrine cell exocytosis. *J. Cell Sci.* **117**, 4739-4748.
Yamasaki, T., Kawasaki, H., Arakawa, S., Shimizu, K., Shimizu, S., Reiner, O., Okano, H., Nishina, S., Azuma, N., Penninger, J. M. et al. (2011). Stress-activated protein kinase MKK7 regulates axon elongation in the developing cerebral cortex. *J. Neurosci.* **31**, 16872-16883.
Yang, T., Sun, Y., Zhang, F., Zhu, Y., Shi, L., Li, H. and Xu, Z. (2012). POSH localizes activated Rac1 to control the formation of cytoplasmic dilation of the leading process and neuronal migration. *Cell Rep.* **2**, 640-651.
Yap, C. C., Vakulenko, M., Kruczek, K., Motamedi, B., Digilio, L., Liu, J. S. and Winckler, B. (2012). Doublecortin (DCX) mediates endocytosis of neurofascin independently of microtubule binding. *J. Neurosci.* **32**, 7439-7453.
Yu, J.-Y., DeRuiter, S. L. and Turner, D. L. (2002). RNA interference by expression of short-interfering RNAs and hairpin RNAs in mammalian cells. *Proc. Natl. Acad. Sci. USA* **99**, 6047-6052.
Zhang, S., Edelmann, L., Liu, J., Crandall, J. E. and Morabito, M. A. (2008). Cdk5 regulates the phosphorylation of tyrosine 1472 NR2B and the surface expression of NMDA receptors. *J. Neurosci.* **28**, 415-424.

Supplementary Fig. S1

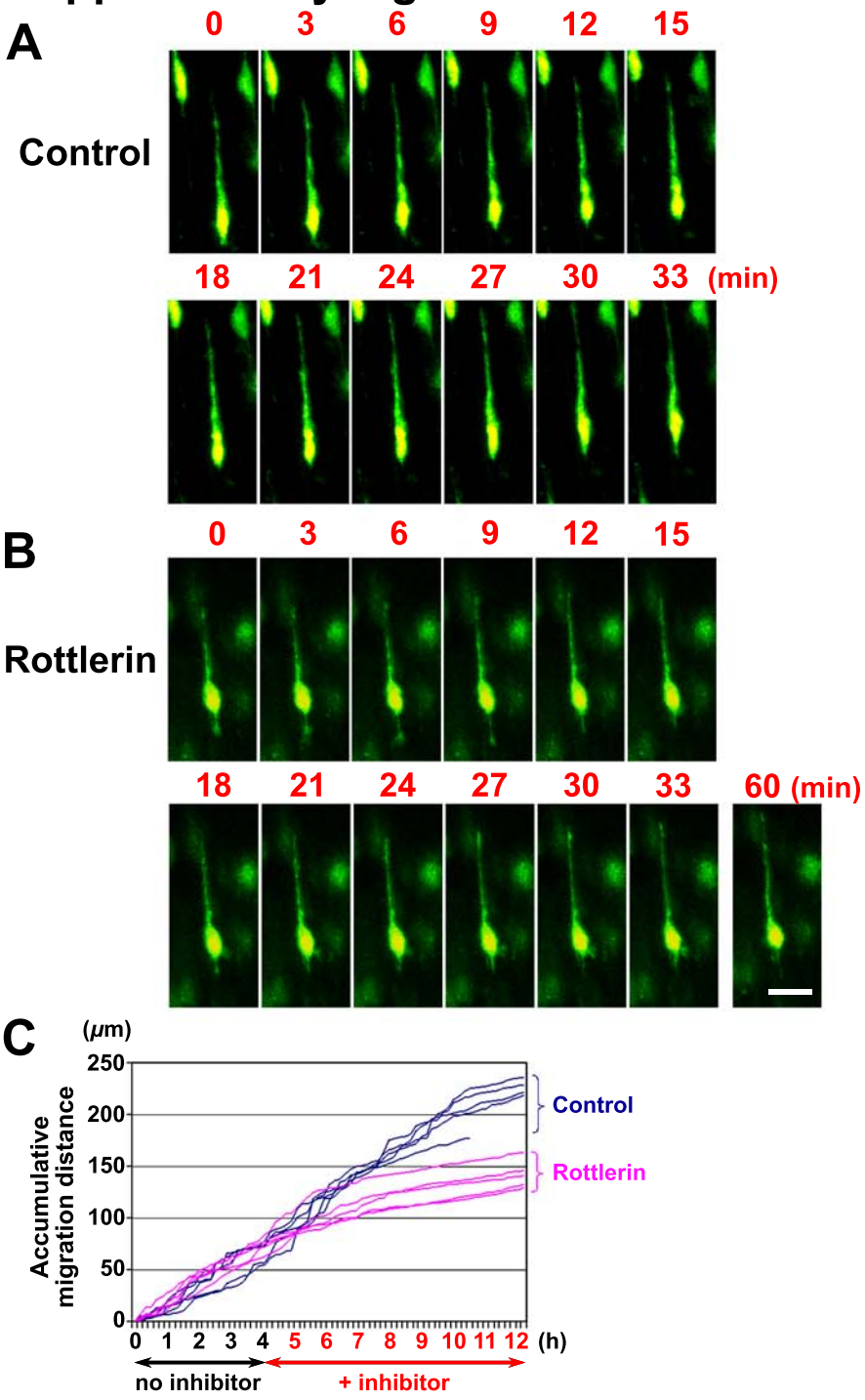

Supplementary Fig. S1. The effects of rottlerin treatment in the locomotion mode of neuronal migration. Time-lapse observation of the locomoting neurons in cultured cortical slices with rottlerin (5 μM) (B) or solvent (A). Mouse cerebral cortices were electroporated with EGFP- and NLS-fused DsRed-expressing vectors at E14, and electroporated brains were subjected to slice culture at E16 with or without rottlerin. High magnification images at 0, 12, 21 and 33 min were extracted for Fig. 1A. At 0 min (shown in red), treatment with an inhibitor had already taken place (time = 0 min: 30 min after inhibitor treatment). (C) Accumulative migration distances of 5 control cells (blue lines) or 5 rottlerin-treated cells (magenta lines). During the first 4 h (shown in black), there was no inhibitor. At 4 h, rottlerin or solvent (control) was added. Scale bar: 20 μm.

Supplementary Fig. S2

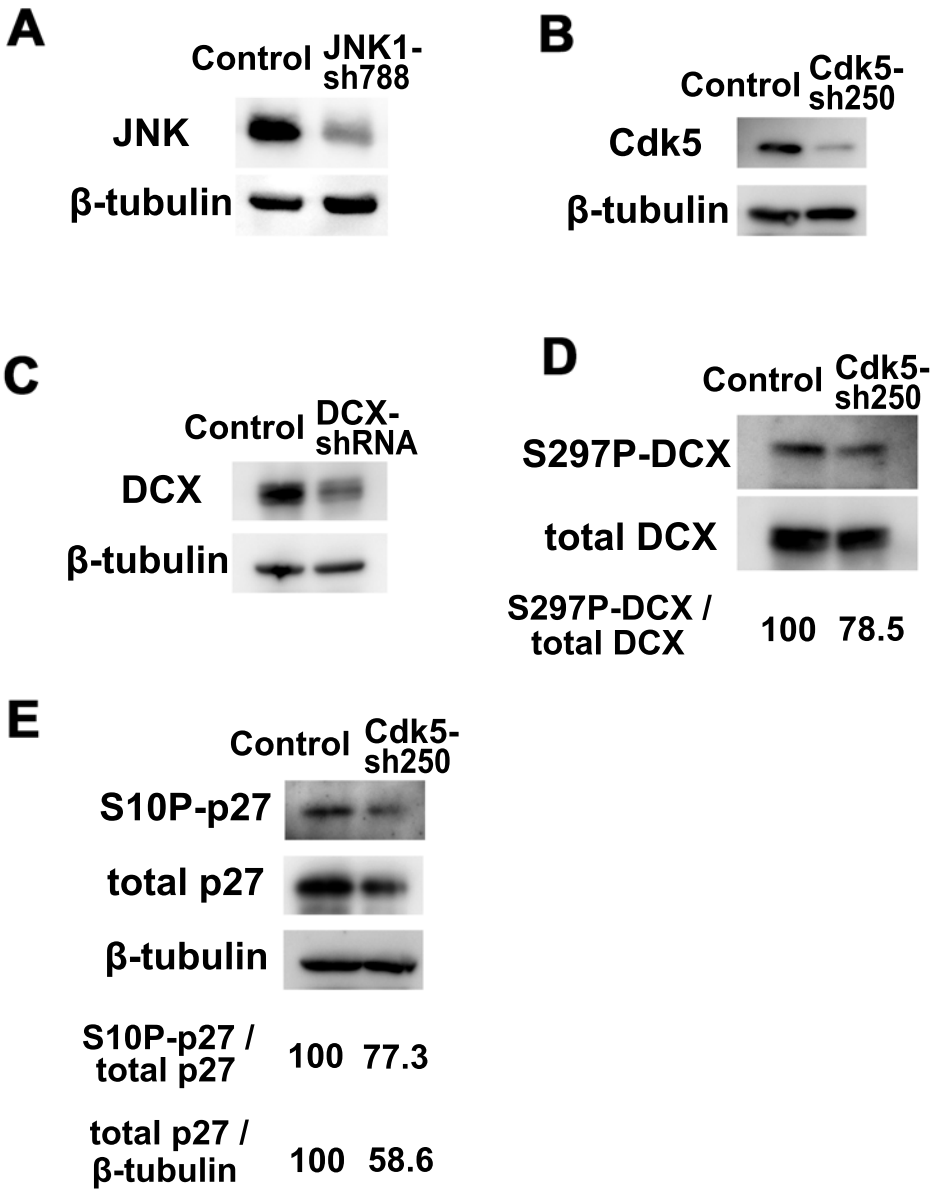

Supplementary Fig. S2. Evaluation of knockdown efficiencies and effects of Cdk5-shRNA on the phosphorylation of DCX and $p27^{kip1}$. (A-C) Amount of JNK1 (A) or Cdk5 (B) or DCX (C) proteins in primary cortical neurons transfected with the indicated shRNA vectors. Primary cortical neurons from E15 cerebral cortices were transfected with the indicated plasmids and incubated for 2 days *in vitro*. Immunoblot analyses of cell lysates with indicated antibodies were performed to evaluate knockdown efficiency. (D,E) Primary cortical neurons from E15 cerebral cortices were transfected with control or Cdk5-knockdown vectors and incubated for 2 days *in vitro*. Immunoblot analyses of cell lysates with indicated antibodies were performed. The numbers indicate the ratio of S297P-DCX/total DCX, S10P-p27/total p27 and total p27/β-tubulin, which were determined by chemiluminescence (LAS-3000mini, FUJIFILM).

Supplementary Fig. S3

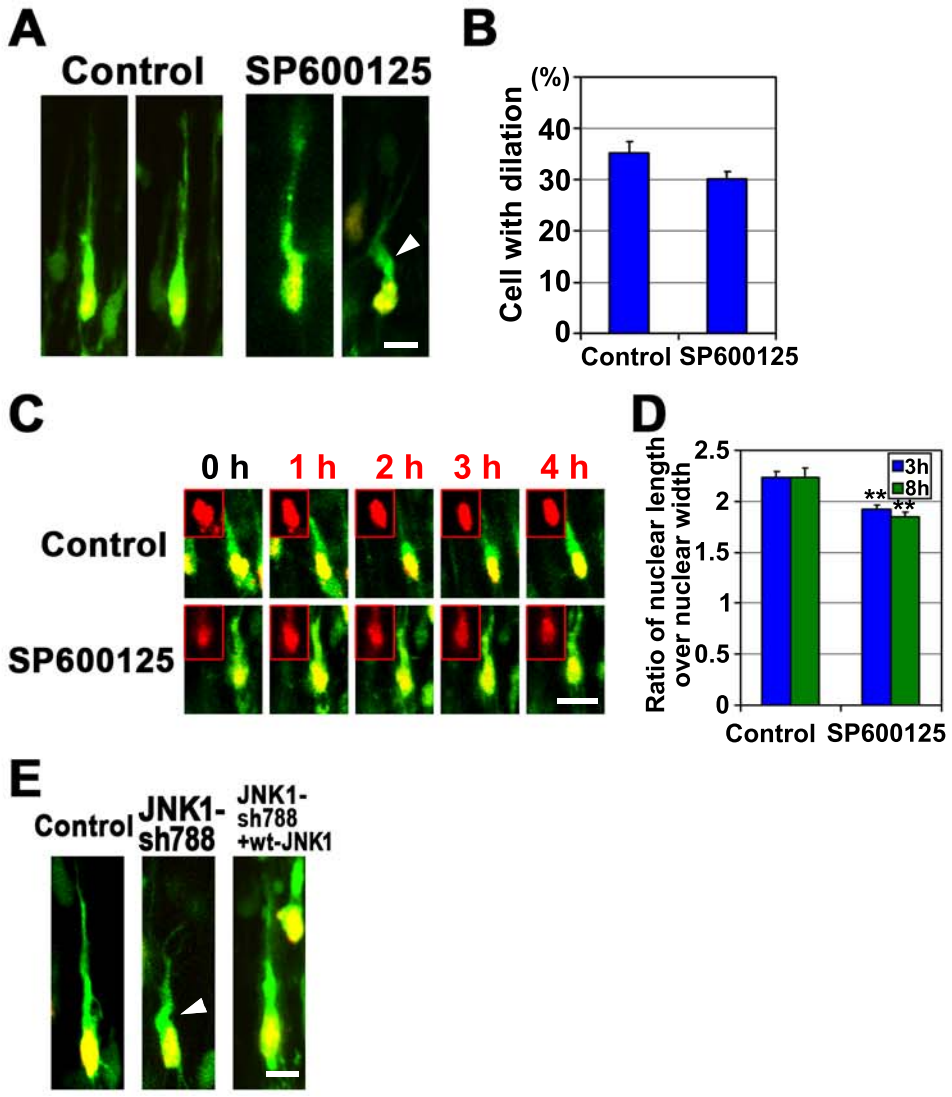

Supplementary Fig. S3. JNK is involved in nuclear morphological changes, but not dilation formation. (A) Two representative images of locomoting neurons in control or SP600125-treated cortical slices. Mouse cerebral cortices were electroporated with EGFP- and NLS-fused DsRed-expressing vectors at E14, and electroporated brains were subjected to slice culture at E16 with or without SP600125. White arrowhead indicates dilation. (B) Ratios of cells with a cytoplasmic dilation 3 h after inhibitor treatment. Data are mean ± s.e.m. Control: *n*=37 cells from four slices, SP600125: *n*=56 cells from five slices. No significant difference between control and inhibitor treatment was found by Student's *t* test. (C) Time-lapse observation of the locomoting neurons in cultured cortical slices with or without SP600125 (50 μM). Cortical slices were treated with the inhibitor just after 0 h. The insets show the nuclear morphologies, visualized by NLS-DsRed-mediated fluorescence. (D) Ratios of length to width of nuclei in locomoting neurons at 3 or 8 h after inhibitor treatment. Data are mean ± s.e.m. Control and SP600125 (3 h and 8 h): *n*=36 cells from three slices. Significance of differences was determined by Student's *t* test. **: $P<0.01$. (E) Representative images of control or JNK1-knockdown or JNK1-knockdown-rescued locomoting neurons. JNK1-knockdown locomoting neurons were able to form the cytoplasmic dilation (arrowhead), but they exhibited abnormal leading process morphologies. Scale bars: 10 μm in A,E; 20 μm in C.

Supplementary Fig. S4

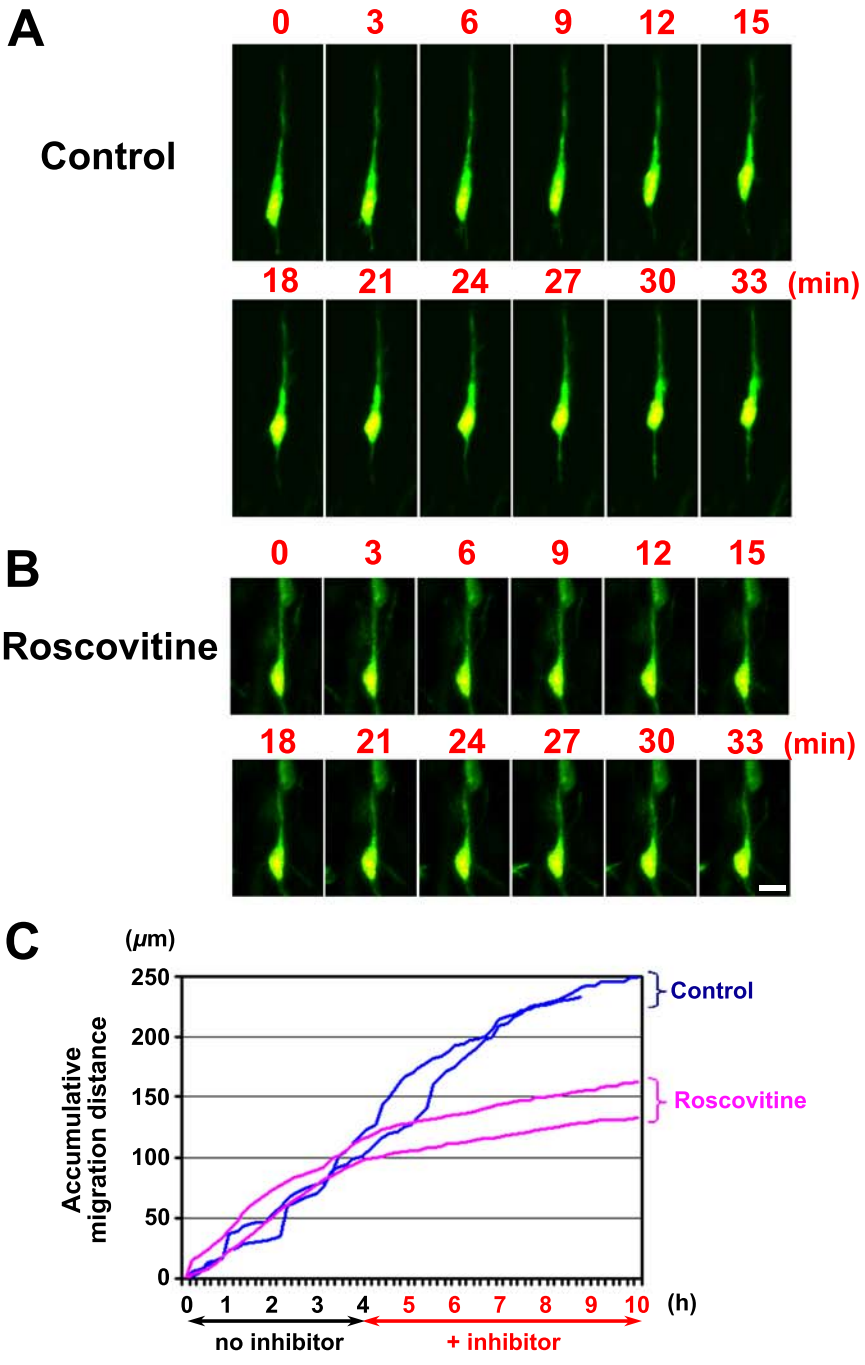

Supplementary Fig. S4. The effects of roscovitine treatment in the locomotion mode of neuronal migration. Time-lapse observation of the locomoting neurons in cultured cortical slices with roscovitine (100 μM) (B) or solvent (A). Mouse cerebral cortices were electroporated with EGFP- and NLS-fused DsRed-expressing vectors at E14, and electroporated brains were subjected to slice culture at E16 with or without roscovitine. High magnification images at 0, 12, 21 and 33 min were extracted for Fig. 2B. At 0 min (shown in red), treatment with an inhibitor had already taken place (time = 0 min: 30 min after inhibitor treatment). (C) Accumulative migration distances of 2 control cells (blue lines) or 2 roscovitine-treated cells (magenta lines). During the first 4 h (shown in black), there was no inhibitor. At 4 h, roscovitine or solvent (control) was added. Scale bar: 20 μm.

Supplementary Fig. S5

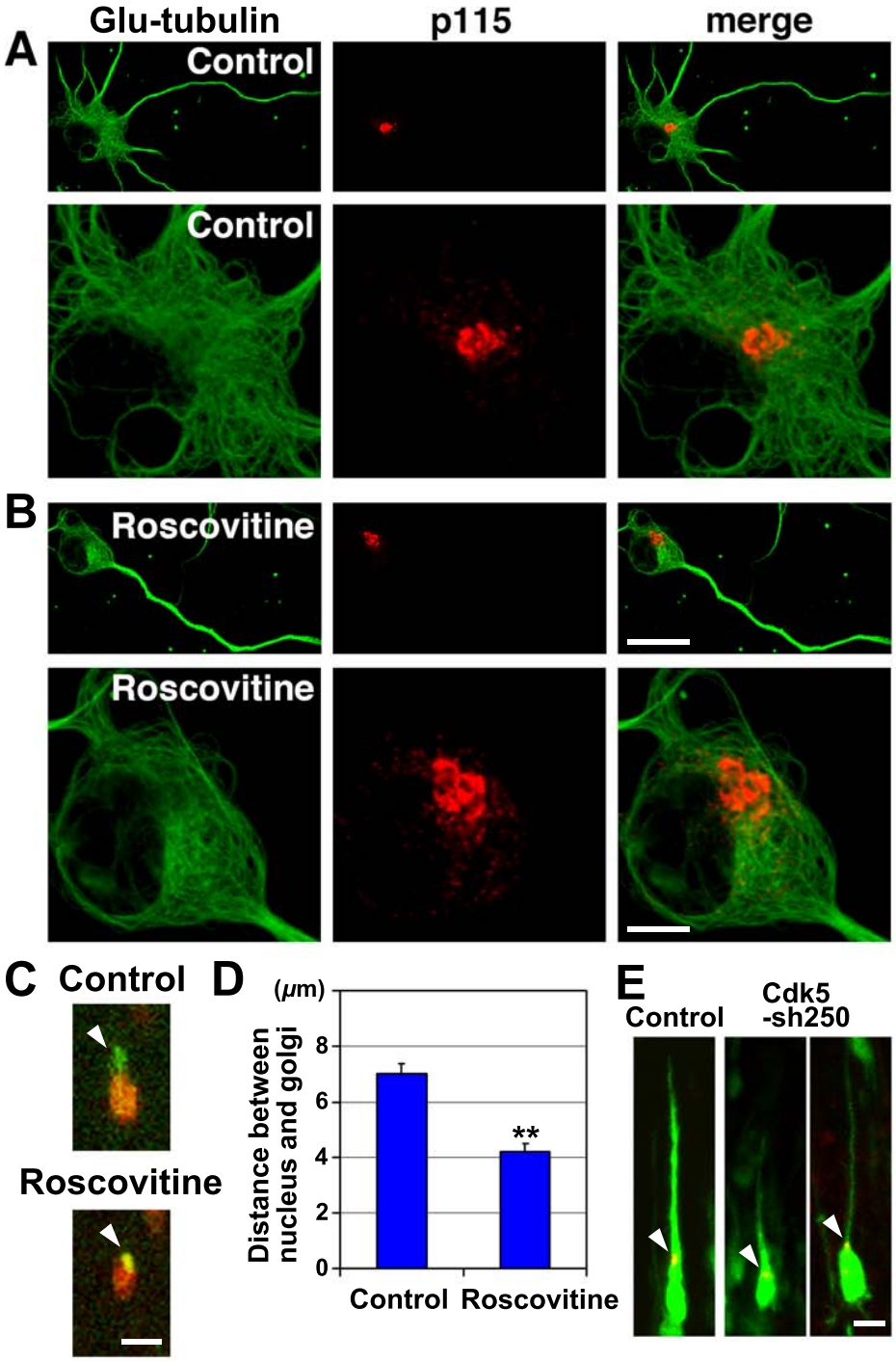

Supplementary Fig. S5. Cdk5 suppression disturbs microtubule morphologies and Golgi localization. (A,B) Primary cortical neurons from E15 cerebral cortices were incubated for 2 days *in vitro* and treated with roscovitine (100 μM) (B) or solvent (A) for 3 h before fixation. Cells were stained with anti-Glu-tubulin (green) and anti-p115, a *cis*-Golgi marker, (red) antibodies. Roscovitine-treated neurons exhibited slightly dispersed Golgi apparatuses. (C) Representative images of locomoting neurons in cortical slices with or without roscovitine (100 μM). Mouse cerebral cortices were electroporated with Golgi-localizing signal-fused EYFP- and NLS-fused DsRed-expressing vectors at E14, and the electroporated brains were subjected to slice culture at E16 with or without roscovitine (100 μM). Arrowheads indicate the Golgi apparatus (green or yellow). (D) The distances between the center of the Golgi and nucleus in the locomoting neurons in cultured cortical slices with or without roscovitine (100 μM). Data are mean ± s.e.m. Control and roscovitine: n=10 cells. Significance of differences was determined by Student's t test. **: P<0.01. (E) Representative images of control or Cdk5-knockdown locomoting neurons. Mouse cerebral cortices were electroporated with EGFP and Golgi-localizing signal-fused DsRed monomer-expressing vectors at E14, and the electroporated brains were subjected to slice culture at E16. Arrowheads indicate the Golgi apparatus (yellow). Scale bars: 20 μm in the upper panels in A and B; 5 μm in the lower panels in A and B; 10 μm in C,E.

Supplementary Fig. S6

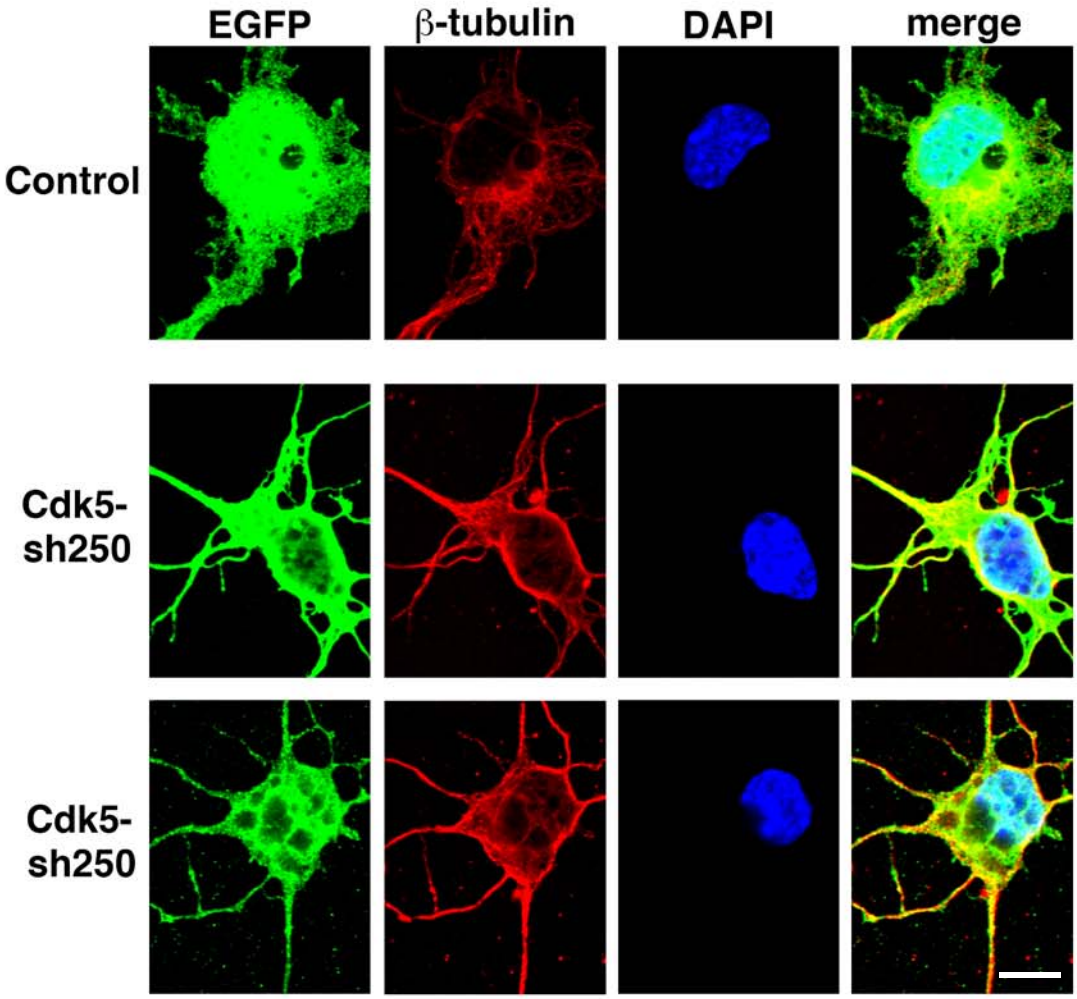

Supplementary Fig. S6. Knockdown of Cdk5 disturbs microtubule morphologies in primary cortical neurons. Primary cortical neurons from E15 cerebral cortices were transfected with the indicated plasmids and incubated for 2 days *in vitro*. Cells were stained with anti-EGFP (green) and anti-β-tubulin (red) antibodies and DAPI (blue) for nuclear staining. The β-tubulin (red) staining signals were extracted for Fig. 5A. Scale bar: 7.5 μm.

Supplementary Fig. S7

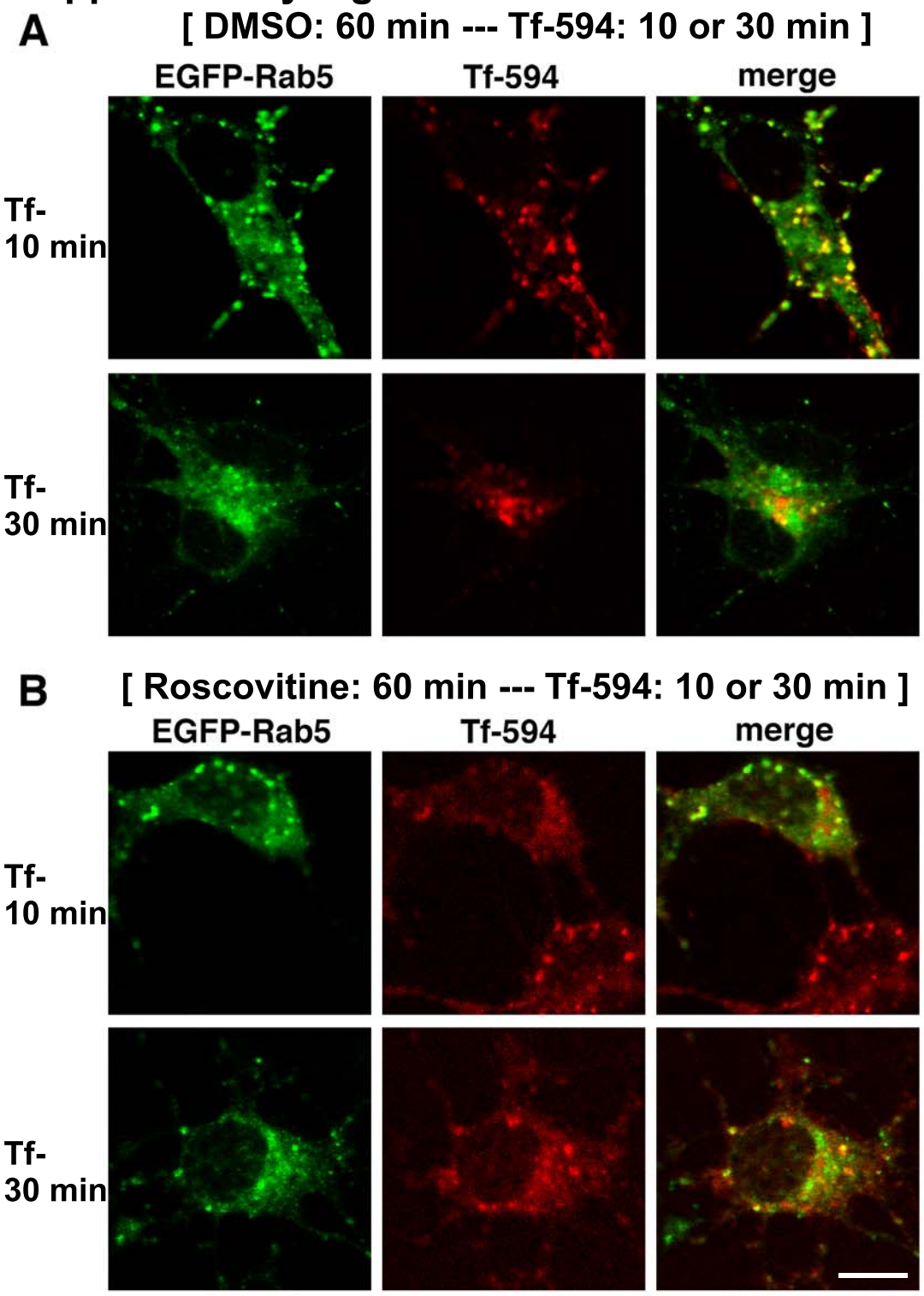

Supplementary Fig. S7. Roscovitine treatment suppresses endocytosis. Primary cortical neurons from E15 cerebral cortices were transfected with EGFP-Rab5-expressing vectors and incubated for 2 days *in vitro*. These cultured cortical neurons were treated with roscovitine (B) or solvent (A) for 60 min, and additionally treated with Alexa594-conjugated transferrin (Tf-594) for 10 or 30 min before fixation. Scale bar: 7.5 μm.

Supplementary Fig. S8

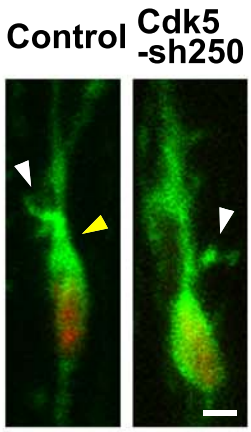

Supplementary Fig. S8. Effects of Cdk5 knockdown on actin organization. Representative images of control or Cdk5-knockdown locomoting neurons. Mouse cerebral cortices were electroporated with EGFP-actin, NLS-fused DsRed, and control or Cdk5-sh250-expressing vectors at E14, and electroporated brains were subjected to slice culture at E16. Accumulation of EGFP-actin signals was observed in the proximal regions of the control locomoting neurons (yellow arrowhead), whereas EGFP-actin was uniformly distributed in the Cdk5-knockdown locomoting neurons. In contrast, both control and Cdk5-knockdown locomoting neurons extended lamellipodia-like structures (white arrowheads). Scale bar: 5 μm.

Supplementary Fig. S9

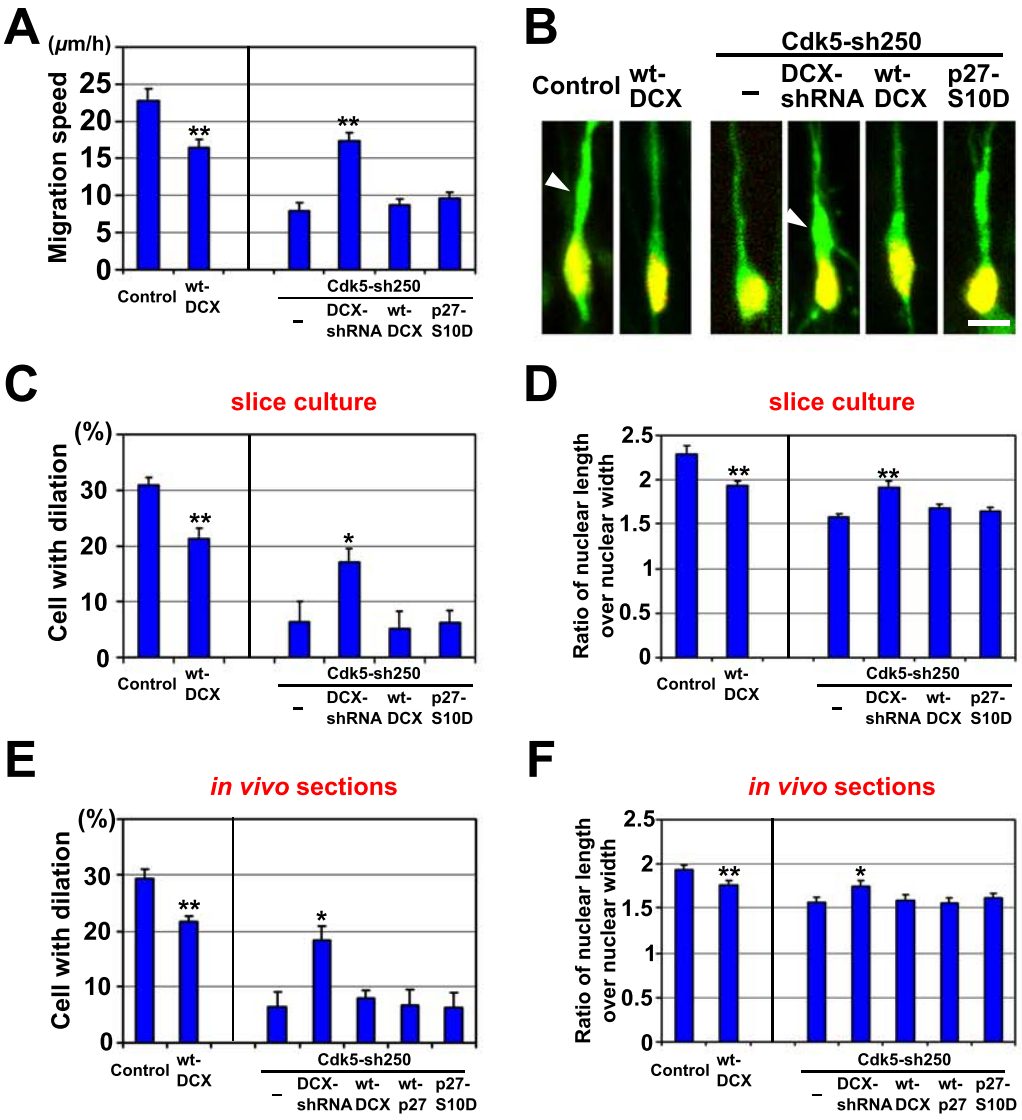

Supplementary Fig. S9. Defects in dilation formation and nuclear elongation of Cdk5-knockdown neurons are partially restored by co-expression of DCX-shRNA. (A) Migration speeds of locomoting neurons were measured in cortical slices electroporated with the indicated plasmids. Control: *n*=10 cells (three slices), wt-DCX: *n*=15 cells (three slices), Cdk5-sh250: *n*=10 cells (four slices), Cdk5-sh250 + DCX-shRNA: *n*=12 cells (three slices), Cdk5-sh250 + wt-DCX: *n*=10 cells (four slices), Cdk5-sh250 + p27-S10D: *n*=14 cells (three slices). (B) Representative images of control or DCX-overexpressing locomoting neurons and those co-electroporated with Cdk5-shRNA and DCX-shRNA or wt-DCX or p27-S10D expressing vectors. (C,E) Ratios of cells with a cytoplasmic dilation in cortical slice cultures (C) or *in vivo* cortical sections (E). Control: *n*=48 cells (four slices), wt-DCX: *n*=89 cells (eight slices), Cdk5-sh250: *n*=33 cells (four slices), Cdk5-sh250 + DCX-shRNA: *n*=53 cells (six slices), Cdk5-sh250 + wt-DCX: *n*=37 cells (four slices), Cdk5-sh250 + p27-S10D: *n*=62 cells (seven slices) in C. Control: *n*=64 cells (five sections), wt-DCX: *n*=74 cells (six sections), Cdk5-sh250: *n*=45 cells (five sections), Cdk5-sh250 + DCX-shRNA: *n*=73 cells (six sections), Cdk5-sh250 + wt-DCX: *n*=74 cells (seven sections), Cdk5-sh250 + wt-p27: *n*=45 cells (six sections), Cdk5-sh250 + p27-S10D: *n*=49 cells (six sections) in E. (D,F) Ratios of length to width of nuclei in locomoting neurons in cortical slice cultures (C) or *in vivo* cortical sections (E). Control, wt-DCX, Cdk5-sh250, Cdk5-sh250 + DCX-shRNA, Cdk5-sh250 + wt-DCX, Cdk5-sh250 + wt-p27 and Cdk5-sh250 + p27-S10D: *n*=30 cells (three slices or three sections). (A,C-F) Data are mean ± s.e.m. Significance of differences was determined by Student's *t* test. *: *P*<0.05, **: *P*<0.01. Scale bar: 10 μm.

Supplementary Fig. S10

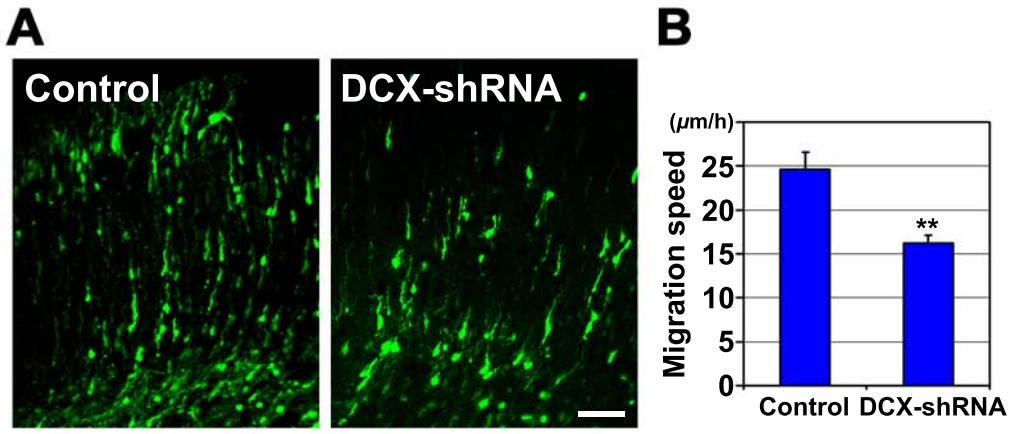

Supplementary Fig. S10. DCX-shRNA reduces the migration speed of the locomoting neurons in cortical slices. (A,B) Migration speeds of locomoting neurons were measured in control- or DCX-shRNA-electroporated cortical slices. In contrast to DCX-mutated human or DCX-shRNA-electroporated rat cerebral cortices where DCX-deficient neurons are stalled in the intermediate zone, most of the DCX-knockdown neurons migrated into the cortical plate in the mouse cortical slices. However, their migration speed was reduced, compared with control. The average migration speed of the DCX-knockdown locomoting neurons was 66% of that of control (control: 24.6±1.9 μm/h, *n*=15 cells. DCX-shRNA: 16.2±0.9 μm/h, *n*=15 cells). This result is consistent with a previous report that the neuronal migration speed in the cortical slices from DCX knockout brains was 69% of that of wild-type brains (Pramparo et al., 2010). (B) Data are mean ± s.e.m. Significance of differences was determined by Welch's *t* test. **: *P*<0.01. Scale bar: 50 μm.

Supplementary Fig. S11

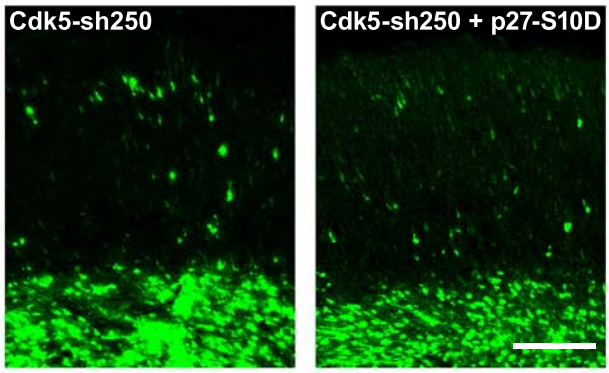

Supplementary Fig. S11. A Ser10-phospho-mimic mutant of $p27^{kip1}$ (p27-S10D) does not rescue the Cdk5-knockdown phenotypes. Mouse cerebral cortices were electroporated with the indicated plasmids at E14, and electroporated brains were harvested and examined at E17. p27-S10D could not restore the multipolar-to-bipolar transition nor dilation formation in Cdk5-knockdown neurons. It is consistent with a previous report that knockdown of $p27^{kip1}$ disturbs the multipolar morphologies, but not multipolar-to-bipolar transition, of migrating neurons, whereas Cdk5 suppression inhibits both multipolar and leading process formation (Kawauchi et al., 2006).
Cdk5 regulates many molecules, including DCX and $p27^{kip1}$ (for dilation formation) (this study), FAK (for nuclear elongation) (Xie et al., 2003) and Ndel1-Lis1 complex (for dynein-dependent nuclear movement) (Niethammer et al., 2000; Tsai et al., 2007) during the locomotion mode of neuronal migration. Furthermore, overexpression of $p27^{kip1}$ also disturbs neuronal migration (Kawauchi et al., 2006). These observations may explain our results that p27-S10D could not rescue the Cdk5-knockdown phenotypes. Scale bar: 100 μm.

Supplementary Movie 1. Time-lapse observation of a control locomoting neuron in cultured cortical slices with solvent (0.1% DMSO). Video was recorded for 75 min with 3 min intervals, using time-lapse confocal microscopy (TCL-SP2, Leica). Green: EGFP, red: NLS-DsRed. The video corresponds to the upper panels of Fig. 1A and supplementary material Fig. S1A. Display rate is 12 fps.

Supplementary Movie 2. The effects of rottlerin treatment in the locomotion mode of neuronal migration. Time-lapse observation of the locomoting neuron in cultured cortical slices with rottlerin (5 mM). Video was recorded for 75 min with 3 min intervals, using time-lapse confocal microscopy (TCL-SP2, Leica). Green: EGFP, red: NLS-DsRed. The video corresponds to the lower panels of Fig. 1A and supplementary material Fig. S1B. Display rate is 12 fps.

Supplementary Movie 3. The effects of roscovitine treatment in the locomotion mode of neuronal migration. Time-lapse observation of the locomoting neuron in cultured cortical slices with roscovitine (100 μM). Video was recorded for 78 min with 3 min intervals, using time-lapse confocal microscopy (FV1000, Olympus). Green: EGFP, red: NLS-DsRed. The video corresponds to the lower panels of Fig. 2B and supplementary material Fig. S4B. Display rate is 12 fps.

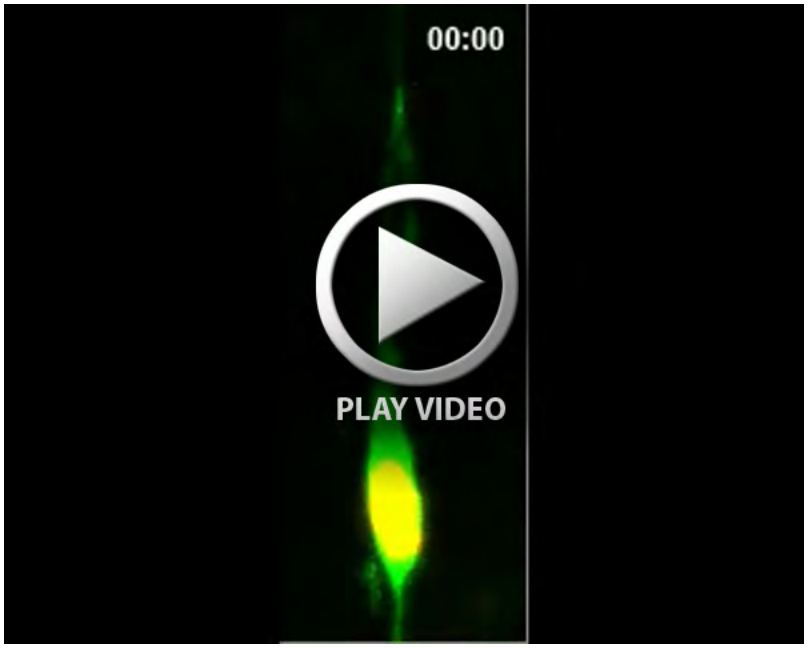

Supplementary Movie 4. The effects of dynasore treatment in the locomotion mode of neuronal migration. Time-lapse observation of the locomoting neuron in cultured cortical slices with dynasore (40 μM). Video was recorded for 78 min with 3 min intervals, using time-lapse confocal microscopy (FV1000, Olympus). Green: EGFP, red: NLS-DsRed. The video corresponds to the lower panels of Fig. 6C. Display rate is 12 fps.

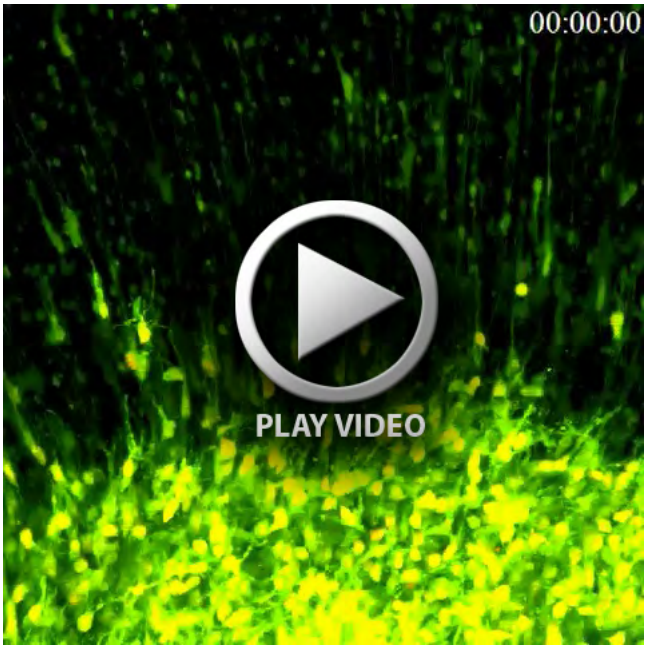

Supplementary Movie 5. The effects of cytochalasin D treatment on the developing cerebral cortex. Time-lapse observation was carried out without any inhibitors during the first 240 min and subsequently with cytochalasin D (10 μM) during the remaining 470 min. Note that inhibition of actin polymerization by cytochalasin D treatment induced the disruption of cortical slice tissues, possibly due to the disturbance of cell-cell adhesions. Video was recorded for 710 min with 10 min intervals, using time-lapse confocal microscopy (TCL-SP2, Leica). Green: EGFP, red: NLS-DsRed. Display rate is 12 fps.

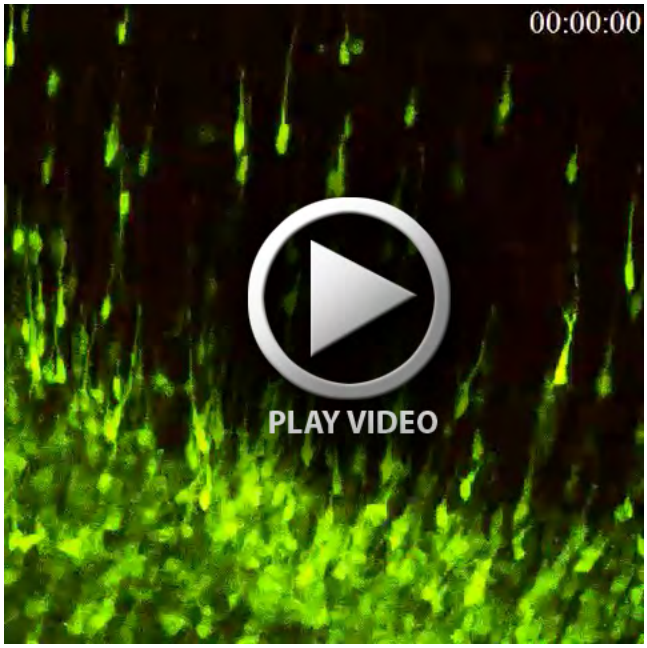

Supplementary Movie 6. The effects of latrunculin B treatment on the developing cerebral cortex. Time-lapse observation was carried out without any inhibitors during the first 240 min and subsequently with latrunculin B (10 μM) during the remaining 470 min. Note that inhibition of actin polymerization by latrunculin B treatment induced the disruption of cortical slice tissues, similar to the cytochalasin D treatment (Supplementary Movie 5). Video was recorded for 710 min with 10 min intervals, using time-lapse confocal microscopy (TCL-SP2, Leica). Green: EGFP, red: NLS-DsRed. Display rate is 12 fps.